[American Journal of Science, Vol. 301, June, 2001, P. 557–592]

A THERMODYNAMIC MODEL FOR Fe-Mg ALUMINOUS CHLORITE USING DATA FROM PHASE EQUILIBRIUM EXPERIMENTS AND NATURAL PELITIC ASSEMBLAGES IN THE 100° to 600°C, 1 to 25 kb RANGE

OLIVIER VIDAL,* TEDDY PARRA, AND FABIEN TROTET

C.N.R.S., UMR 8538, E.N.S.-Laboratoire de Géologie, 24 rue Lhomond, 7500 Paris, France

ABSTRACT. The purpose of this study is to derive a solid solution model for aluminous (Si < 3 a.p.f.u.) chlorites encountered in metapelites over a wide range of P-T conditions. A compilation of chlorite compositions in quartz-bearing rocks led us to propose a four-thermodynamic-component (Mg-amesite, clinochlore, daphnite, and Mg-sudoite) solid solution model that accounts for the Tschermak, Fe-Mg, and di/trioctahedral substitutions observed in nature. A new feature emerging from this compilation is the contrasting effect of temperature and pressure variations on the Al^{IV} and vacancy contents in chlorites. A 3-site mixing model with symmetric Margules parameters and ideal inter-site interaction has been adopted to model these compositional changes. In contrast to previous models, the relevant thermodynamic data (Mg-amesite and daphnite standard state properties as well as W_{AlMg}, W_{AlFe}, $W\square_{Fe}$, $W\square_{Mg}$, and $W\square_{Al}$ on M1) are calibrated with independent sets of published experiments conducted in the MASH and FMASH systems (~60 reversals) as well as about 200 natural data involving chlorite + quartz ± (carpholite or chloritoid) assemblages. Moreover, the constraints span a wide range of pressure and temperature conditions (100°-850°C, 0.5-20 kb), so that no extrapolation outside the calibration range is needed for P-T thermobarometric purposes. The calculated thermodynamic data are compatible with the thermodynamic data of clinochlore from Berman (1988), Mg-sudoite and Mg-carpholite data from Vidal and others (1992), Fe-chloritoid from Vidal and others (1994), and the chlorite-chloritoid Fe-Mg exchange thermometer of Vidal and others (1999). The chlorite solution model seems to be consistent also with the solid solution properties from Berman (1990) for garnet, Fuhrman and Lindsley (1988) for plagioclase, and Evans (1990) for epidote, although additional work is required to explain the large discrepancies observed between the temperatures obtained from empirical garnet-chlorite Fe-Mg exchange thermometers and the temperatures calculated in the present study.

The use of several chlorite endmembers makes the estimation of paleo-pressure and -temperature conditions possible for high-variance parageneses (> 1) which is not possible when using only one chlorite endmember (classically clinochlore). In particular, reliable pressure estimates can be made for the common chlorite-quartz-carpholite or chloritoid or garnet bearing rocks devoid of aluminosilicates, whereas such estimates are impossible when using only one chlorite endmember. In the most favorable cases, temperature conditions can be estimated from the location of the temperature-dependent equilibrium 2 clinochlore + 3 Mg-sudoite = 4 Mg-amesite + 7 quartz + 4 H_2O, that is from the composition of chlorite associated with quartz. Our chlorite solution model predicts that at fixed pressure and $(XMg)_{chlorite}$, the location of this equilibrium is shifted toward higher temperature when decreasing the Si, Al^{VI}, and vacancy contents and increasing the Al^{IV} content. This result is compatible with the classical empirical thermometers based on the Al^{IV} and vacancy contents in chlorite. However, the calculated effect of pressure is an increase of the Al^{IV}, Al^{VI}, and vacancy contents. This explains why the empirical chlorite thermometers (based on the Al^{IV} contents in chlorite) derived from low-T samples cannot be used at high pressure conditions.

*Present address: Universite J. Fourier, LGCA (UMR5025), 1381, rue de la piscine, BP53, 38041 Grenoble cedex 9, France.

INTRODUCTION

Chlorite is common in a great variety of rocks and geological environments. It displays a wide range of chemical compositions that reflect its physicochemical conditions of formation. Therefore, chlorite presents an interesting potential for thermobarometric estimates.

Two approaches have been proposed to use the compositional variability of chlorite to determine the thermobarometric conditions prevailing during its formation: (1) the use of empirical calibrations based on the tetrahedral aluminium occupancy as a function of measured temperature in geothermal systems (Cathelineau and Nieva, 1985; Cathelineau, 1988; Kranidiotis and MacLean, 1987; Jowett, 1991; Hillier and Velde, 1991; among others), and (2) thermodynamic calculation of equilibrium conditions for chlorites whose composition is expressed as a linear combination of a set of endmember components of known thermodynamic properties. The mixing properties between these endmembers are either calibrated using experimental data (McPhail and others, 1990; Holland and others, 1998) obtained at high temperature (> 500°C) in the simplified MgO-Al_2O_3-SiO_2-H_2O (MASH) chemical system or derived assuming ideal mixing for cations on energetically equivalent sites (Walshe and Solomon, 1981; Walshe, 1986).

Because of its simplicity, the first approach has been increasingly used in diagenetic settings in recent years. However, studies aimed at identifying the chlorite composition variations with P and T indicate that chlorite compositions are not only sensitive to conditions of metamorphism but also to bulk rock composition (Zane and Sassi, 1998). Moreover, significant variations of composition can occur among chlorites coexisting in the same hand sample or even in the same thin section. This reflects the fact that different specific assemblages drive the substitutions in different directions with changing P and T. Consequently, empirical methods based on the composition of chlorite alone cannot provide reliable P-T estimates. Furthermore, the application of such empirical thermometers is restricted to temperatures (below 300°C), rock mineralogies, and compositions at which they were calibrated. For these reasons, various equations based on different rock compositions have been proposed, but none of them gives reliable results over a wide range of physicochemical conditions of crystallization (DeCaritat and others, 1993).

The use of thermodynamics is an improvement to the empirical thermometer, since it accounts for the variations of the rock mineralogy and the potential influence of additional thermophysical parameters (that is fluid composition or redox conditions, Walshe and Solomon, 1981; Walshe, 1986). However, none of the models published to date is able to account for the composition of chlorite observed from low-grade metamorphism to its breakdown temperature conditions (about 850°C at 15 kb in MASH; Baker and Holland, 1996). The solution components used by Walshe (1986) account for the relevant substitutions observed in natural chlorite, including $FeMg_{-1}$ (FM), Tschermak (TK), and di-trioctahedral (DT) substitutions, but the thermodynamic data and activity-composition model are not constrained by the P-T-composition relations observed at $T > 400$°C and $P > 5$ kb in either experimental systems or in nature. Conversely, thermodynamic data and solution models extracted from experiments do not account for all substitutions observed in natural chlorites. McPhail and others (1990) calculated thermodynamic properties for an Al-free trioctahedral chlorite of Mg-serpentine composition (ChlS: $Si_4(Mg)_6O_{10}(OH)_8$) and for Mg-amesite (Mg-Am:$Si_2Al_4Mg_4O_{10}(OH)_8$) which allows the extent of TK substitution with P-T conditions to be modeled in the experimental MASH system but not the extent of FM and DT substitutions observed in nature. Holland and others (1998) proposed a non-ideal activity model accounting for the compositional and possible ordering variations (reciprocal solutions) among four endmembers (Mg-Am, ChlS,

clinochlore (Clin: $Si_3Al_2Mg_5O_{10}(OH)_8$), and daphnite (Daph: $Si_3Al_2Fe_5O_{10}(OH)_8$)), but the activity model assumes that the chlorite composition can be represented by the simple formula $Si_{4-x}Al_x(Mg, Fe)_{6-x}Al_xO_{10}(OH)_8$. This model only pertains to chlorites devoid of octahedral vacancies (that is, no DT substitution) for which $Al^{IV} = Al^{VI}$. However, the amount of octahedral vacancies in chlorites can be significant in rocks metamorphosed at $T < 450°C$ (see below).

The purpose of this study is to derive a solid solution model and thermodynamic data for chlorite endmember components (1) able to handle variable octahedral site occupancies independent of TK substitution and (2) that can be used to calculate the conditions of equilibrium for the most common natural chlorites encountered in metapelites, mafic, and felsic rocks over a wide range of P-T conditions, that is, chlorite with a Si content < 3 a.p.f.u. (Laird, 1988). The restriction of the model to such compositions avoids the problems related to reciprocal solutions (Holland and others, 1998). In contrast to previous models, we attempt to constrain the relevant thermodynamic data with independent sets of published experiments conducted in the MASH and FMASH systems (300°-850°C, 0.5-25 kb) as well as various natural data from rocks of different grade.

compositional variability of chlorite in aluminous (meta)pelites

Relevant Chlorite Substitutions

Three main substitutions occur in chlorite, all of which depend on the P and T conditions as well as on the rock chemistry (or, at fixed P and T conditions, on the mineralogy). The $FeMg_{-1}$ substitution (FM) extends over the whole range between Mg and Fe endmembers, the coupled Tschermak substitution (TK: $Al^{IV}Al^{VI}Si_{-1}(Mg,Fe)_{-1}$) is restricted to chlorite compositions between Clin-Daph and Am in aluminous metapelites, and the di/trioctahedral substitution (DT) corresponds to the coupled exchange of Mg and Fe for Al in the 2:1 layer (from the (Clin/Daph)-Am binary toward the sudoite (Sud: $Si_3Al_4(Mg,Fe)_2\square O_{10}(OH)_8$) component, fig. 1). To insure charge balance, three (Mg, Fe^{2+}) are involved for two Al^{3+}, leading to the formation of one vacancy ($(Mg,Fe^{2+})_3\square_{-1}Al_{-2}$).

It is difficult to derive the extent of the DT substitution from electron-microprobe analyses (EMPA), because vacancies are not a measurable quantity. Defining the proportion of vacancies is equivocal and depends on the reference used to normalize the microprobe analyses to the structural formula (Laird, 1988). In particular, the proportion of calculated vacancies depends on the amount of Fe^{3+}, which is also not assessed by EMPA. A second problem arises from the possible interstratification of chlorite with other sheet silicates which might also lead to erroneous structural formulae (Jiang and others, 1994). For these reasons, Jiang and others (1994) claimed that vacancies calculated from EMPA are an artifact. However, it is generally accepted that Fe^{3+} in chlorite-group minerals is controlled by crystallochemical constraints rather than by fO_2 conditions and is never abundant (Cooper, 1972; Black, 1975; Shirozu, 1978; Dyar and others, 1992; Nelson and Guggenheim, 1993; Zane and Sassi, 1998). Moreover, octahedral contents lower than six are also observed in low temperature chlorites devoid of significant smectite or mica contamination ($K+Na+Ca < 0.05$ a.p.f.u.). In metapelites that generally have a high ($Fe/Fe+Mg$) ratio, the formation of chlorite is favored instead of smectites or corrensite, and there is no important interlayering of chlorites with other sheet-silicates (Ernst and others, 1970; Ahn and Peacor, 1985; Curtis and others, 1985; Leoni and others, 1998). Therefore, octahedral vacancies in chlorites should be a real feature at $T < \sim 300°C$, $P < 1$ kb (McDowell and Elders, 1980; Cathelineau and Nieva, 1985; Cathelineau, 1988; Hillier and Velde, 1991; DeCaritat and others, 1993; Leoni and others, 1998).

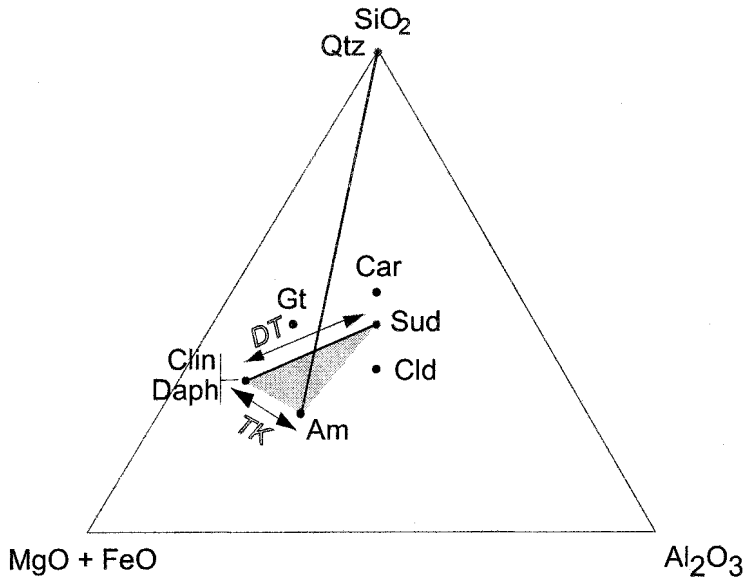

Fig. 1. Si-Al-Mg +Fe ternary for representation of the chlorite endmembers and substitutions considered in the chlorite model (for the range of composition corresponding to the gray area). TK : Tschermak substitution; DT : di/trioctahedral substitution. The chlorite + quartz stability conditions can be computed from the reaction Clin + Mg-Sud = Mg-Am + Qtz (equilibrium 4), as indicated by the intersecting tie-lines. Sud : sudoite; Clin : clinochlore; Am : amesite; Daph : daphnite; Car : carpholite; Gt : garnet; Cld : chloritoid, Qtz : quartz.

In the following, we assume that the incorporation of octahedral vacancies results only from the DT substitution. Following this assumption, the number of vacancies (□) is proportional to the difference between octahedral and tetrahedral aluminum obtained from the structural formula calculated on a 14 anhydrous oxygen basis, assuming all iron to be divalent ($\square = (Al^{VI}\text{-}Al^{IV})/2$). Any significant difference between □ and $(Al^{VI}\text{-}Al^{IV})/2$ is considered to be indicative of the presence of Fe^{3+} or contamination. Such analyses were not considered in the present study (see below).

Influence of P-T Conditions on the Extent of Tschermak and Di/trioctahedral Substitutions

Above ~300°C, the proportion of octahedral vacancies in low pressure environments (< 1 kb) is predicted to be 0 (Cathelineau and Nieva, 1985). However, Leoni and others (1998) showed that vacancies are still present at temperatures above 300°C in chlorites from pelites metamorphosed at higher pressure conditions. The competing effect between temperature and pressure upon the proportion of vacancies in chlorites is depicted in figure 2, which shows the molar fractions of (Clin + Daph), Am and Sud (XClin + XDaph + XAm + XSud =1, no negative Xi) in chlorites occurring with quartz ± carpholite or chloritoid at various P-T conditions (see app.). All the chlorite analyses used to construct figure 2 have a (Cr +Ca + Na + K) content < 0.07 a.p.f.u.. At low pressure, the molar fraction of sudoite (XSud = □) is effectively negligible at T above 300°C. It increases rapidly in the 300° to 400°C range, with an increase of pressure from < 1 to 3-7 kb. At high pressure conditions, XSud also decreases with temperature, but it is negligible (XSud < 0.05) at higher temperature (475°C at 10 kb or 550°C at 15 kb). Therefore, the □ = f(T) equation derived by Cathelineau and Nieva (1985) from low-temperature samples (dashed line in fig. 2) is shifted to higher temperature in the case of higher-pressure chlorite samples from chloritoid- or carpholite-bearing rocks.

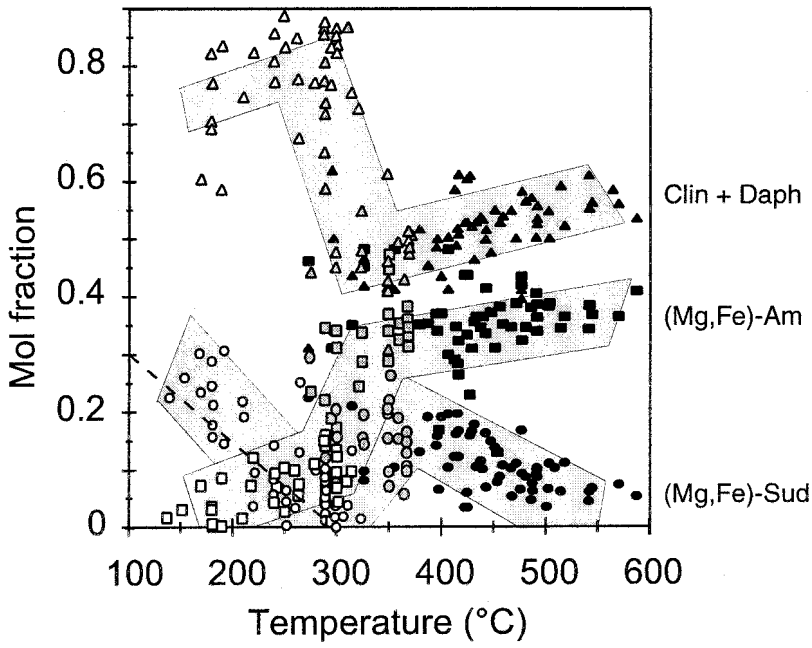

Fig. 2. Molar fractions of (Fe,Mg)-sudoite (circles), (Fe,Mg)-amesite (squares), and (clinochlore + daphnite) (triangles) in chlorites formed in quartz-bearing rocks at $P < 2$kb, $T < 350$°C (white symbols), $2 < P < 7$ kb, $250 < T < 375$°C (gray symbols) $9 < P < 16$ kb, $350 < T < 575$°C (black symbols) as a function of temperature. The composition and original temperatures are listed in the appendix. The dashed line indicates the empirical $\square = f(T)$ relation proposed by Cathelineau and Nieva (1985).

Figure 2 also shows that large variations in the clinochlore + daphnite (XClin + XDaph) and amesite (XAm) molar fractions are associated with P and T variations. At pressure below 1 kb, $0 < XAm < 0.15$ and $0.7 < XClin + XDaph < 0.85$, whereas at pressure above 10 kb, $0.3 < XAm < 0.4$ and $0.45 < XClin + XDaph < 0.6$. In both pressure domains, XClin + XDaph and XAm gently increase with increasing temperature. These trends correspond to a decrease in Si, Al^{VI}, and $\square$ and an increase in Al^{IV} and (Fe + Mg) with increasing temperature. The pressure effects correspond to a Si and (Fe + Mg) decrease and an increase of Al^{IV}, Al^{VI}, and $\square$. Figure 2 also indicates that XAm, XSud, and (XClin + XDaph) = f(T) empirical relations (or similar relations based on the corresponding Si, Al^{VI}, and $\square$ content) calibrated from low-P samples cannot be used at P above 3 to 4 kb. In contrast, the chlorite thermodynamic model is expected to account for the observed XAm, XSud, and (XClin + XDaph) = f(P,T) trends.

CHLORITE SOLUTION MODEL

At least four thermodynamic endmembers are required to model the TK, FM, and DT chlorite solid solutions. Since the present study focuses on chlorite with Si < 3 a.p.f.u., chlorite compositions are approximated within the system clinochlore, daphnite, Mg-amesite, Mg-sudoite. Two groups of tetrahedral sites ($(T1)_2$ and $(T2)_2$) and two groups of octahedral sites (M1,M4 and $(M2)_2$, $(M3)_2$) have been identified in chlorites (Bailey, 1988, and references therein). We distribute cations among the different sites (table 1) following Holland and others (1998), whereby octahedral Al in trioctahedral chlorite is restricted to the octahedral M1 and M4 sites with a strong preference for M4, and tetrahedral Al is restricted to T2 on which it substitutes

TABLE 1

Thermodynamic endmember atomic site partition and method used to calculate the atomic site partition in chlorite of intermediate composition

	$(T1)_2$	$(T2)_2$	M1	$(M2+M3)_4$	M4
Clin	$(Si)_2$	Si Al	Mg	$(Mg)_4$	Al
Daph	$(Si)_2$	Si Al	Fe	$(Fe)_4$	Al
Mg-Am	$(Si)_2$	$(Al)_2$	Al	$(Mg)_4$	Al
Mg-Sud	$(Si)_2$	Si Al	□	$(Al)_2(Mg)_2$	Al
			Atom site distribution		
□	0	0	[1] $(Al^{VI}-Al^{IV})/2$	0	0
Fe + Mg	0	0	[3] $(Fe + Mg)_{tot} - (Fe + Mg)_{M2+M3}$	[2] $4 - (Al^{VI}-Al^{IV})$	0
Mg	0	0	[4] $XMg*(Fe + Mg)_{M1}$	[5] $Mg_{tot} - Mg_{M1}$	0
Fe	0	0	[6] $(1 - XMg)*(Fe + Mg)_{M1}$	[7] $Fe_{total} - Fe_{M1}$	0
Al	0	Al^{IV}	[8] $1-(Fe+Mg + □)_{M1}$	[1] $Al^{VI}-Al^{IV}$	1

[1] to [8] indicate the sequence in which the cation assignments are made, tot: total from the structural formula, $XMg = Mg_{tot}/(Mg_{tot} + Fe_{tot})$, □: vacancies.

randomly for Si. In addition, we assume that (1) vacancies in sudoite are restricted to the M1 site, (2) Fe, Mg, and Al mix randomly over the (M2 + M3) sites, and (3) there is no Mg to Fe partitioning between M1 and (M2 + M3) (that is, equal Mg/Fe proportions in these sites). The cation site distribution obtained with these assumptions is illustrated in table 1. It is emphasized that □ is calculated from the difference $(Al^{VI} - Al^{IV})$ and that $(Al)_{M1}$ is obtained from $(Fe+ Mg + □)_{M1}$. Consequently, the atomic site distribution calculation reported in table 1 can only be applied to chlorites whose composition is a linear combination of clinochlore, daphnite, amesite, and sudoite endmembers (all positive). In addition to the relations listed in table 1, the following two equations must be verified : $(Al^{VI} - Al^{IV})/2 = □_{M1} = 6 -$ octahedral cations and $(Al)_{[M1 + M2 + M3 + M4]} = Al^{VI}$. However, analytical uncertainties may lead to some deviation from the ideal case. For this reason, chlorite compositions used as input data for the thermodynamic data extraction and application examples must meet the following criteria:

$$(Al)_{[M1+M2+M3+M4]} = Al^{VI} \pm 3 \text{ percent} \quad (1)$$

$$(Al^{VI} - Al^{IV})/2 = 6 - \text{octahedral cation sum (from the structural formula)} \pm 15 \text{ percent} \quad (2)$$

This two criteria were used to reject analyses that cannot be expressed as a linear combination of (Fe,Mg)-amesite, (Fe,Mg)-sudoite, clinochlore, and daphnite (no negative component).

Formalism

A 3-site mixing model with symmetric Margules parameters and ideal inter-site interaction has been adopted to model chemical exchange in chlorite. The formalism used in this study to calculate the endmember standard state thermodynamic proper-

ties and the mixing parameters is similar to that described by Berman and Brown (1984) and Mäder and others (1994).

For any balanced chemical reaction involving j phase components, the equilibrium condition is:

$$0 = \sum_j v_j \Delta_a G_j^{P,T} - RT \ln K \tag{3}$$

where v_j is the stoichiometric reaction coefficient, $\Delta_a G^{P,T}$ is the apparent Gibbs free energy of formation (Berman, 1988), and K is the equilibrium constant, which can be written as

$$K = \prod_j (a_{ideal}\gamma)_j^{v_j} \tag{4}$$

where a_{ideal} is the ideal (configurational) part of the activity, and γ is the activity coefficient accounting for non-ideal contributions.

$$(a_{ideal})_j = \prod_s \prod_m \left(\frac{ns}{r_m} Xm\right)^{r_m} \tag{5}$$

where ns is the multiplicity of site s, r_m and Xm are the number and the mole fraction respectively of cation m on site s. For the symmetric interactions assumed in this study, γ_m is computed from:

$$n_s \cdot R \cdot T \cdot \ln \gamma_m = \sum W_{ij} \cdot X_i \cdot X_j \cdot \left[\frac{Q_m}{X_m} - 1\right] \tag{7}$$

where W_{ij} is the Margules parameters, and Q_m is the number of i, j subscripts equal to m (0 or 1).

Eq (3) can be rearranged to compute the unknown thermodynamic parameters for known P and T conditions and known mineral compositions. Molar volumes, heat capacity, expansivity, and compressibility terms for all chlorite endmembers were either taken from the literature or estimated (table 2). Thermodynamic data for clinochlore and other minerals considered in the following were taken from the updated data set (Jan92) of Berman (1988).

The input data discussed below are insufficient to derive a unique estimate of each solution parameter for all possible interactions on each site (table 1). For this reason, W_{AlSi} has been arbitrarily set to zero. W_{FeMg} is also assumed to be zero which is consistent with the value (~4 kJ) predicted by the model of Davies and Navrotsky (1983) and is probably within error of zero (Holland and others, 1998). Lastly, the W_{AlMg} and W_{AlFe} parameters on (M2 + M3) are also set to zero because the amount of $Al_{(M2+M3)}$ is low and the possible non-ideality of the DT substitution is monitored by the □-Al, -Fe, and -Mg interactions on M1. Therefore, the remaining adjustable Margules parameters are W_{AlMg}, W_{AlFe}, $W\square_{Fe}$, $W\square_{Mg}$, *and* $W\square_{Al}$ on M1, and the adjustable standard state properties are the enthalpy and third-law entropy of Mg-amesite, daphnite, and Mg-sudoite. The ideal part of the clinochlore, daphnite, Mg-amesite, and Mg-sudoite activities computed from eq (5) are:

$$a_{Daph} = 4X_{Si}^{T2} X_{Al}^{T2} X_{Fe}^{M1} (X_{Fe}^{(M2+M3)})^4$$

$$a_{Clin} = 4X_{Si}^{T2} X_{Al}^{T2} X_{Mg}^{M1} (X_{Mg}^{(M2+M3)})^4$$

$$a_{Mg-Sud} = 64X_{Si}^{T2} X_{Al}^{T2} X_{\square}^{M1} (X_{Al}^{(M2+M3)})^2 (X_{Mg}^{(M2+M3)})^2$$

$$a_{Mg-Am} = (X_{Al}^{T2})^2 X_{Al}^{M1} (X_{Mg}^{(M2+M3)})^4$$

TABLE 2

298K, 1 bar thermodynamic data calculated in this study (see Berman, 1988 for the format)

	H°f J/mol	S° J/mol/K	V° J/bar	k0	k1	$k2.10^{-2}$	$k3.10^{-3}$	$v3.10^{5}$ K^{-1}	$v4.10^{9}$ K^{-2}	$v1.10^{6}$ bar^{-1}	$v2.10^{8}$ bar^{-2}
Daphnite	-7120845	559.4	21.588*	1229.23**	-10256.5**	-122769**	2121510**	2.6451***	0.00***	-1.819471***	0.0***
Mg-Amesite	-9035900.5	403.2	20.520†	1144.45**	-8327.2**	-200580**	2820786**	2.6451***	0.00***	-1.819471***	0.0***
Mg-chloritoid	-3557301	132	6.864	399.52**	-2538.5**	-63616**	489510**	3.0000‡	0.00‡	-0.675676‡	0.0‡

Chlorites (M1)	*WH*	*WS*	*WV*
AlMg	-9400	-30	-0.2
AlFe	12000	35	-0.5
□Al	-10000	-30	0.9
□Fe	2000	-15	0.4
□Mg	5000	-25	0.9
Garnet	GE0-Calc JAN92 data base		
Chloritoid	Ideal		
Carpholite	Ideal		

Sources: *, estimated by Vidal and others (1999); **, estimated according to Berman and Brown (1985); ***, same as clinochlore from Berman (1988); †, Baker and Holland (1996); ‡, Comodi and others (1992)

According to the assumptions discussed above, the activity coefficients of the same endmembers are derived from the following expressions computed from eqs (6) and (7):

$$RT\ln\gamma_{Clin} = (Al-MgAl)W_{AlMg} - FeAlW_{AlFe} + (\square - \square Mg)W_{\square Mg} - \square AlW_{\square Al} - \square FeW_{\square Fe}$$

$$RT\ln\gamma_{Daph} = -MgAlW_{AlMg} + (Al-FeAl)W_{AlFe} - \square MgW_{\square Mg} - \square AlW_{\square Al} + (\square - \square Fe)W_{\square Fe}$$

$$RT\ln\gamma_{Sud} = -MgAlW_{AlMg} - FeAlW_{AlFe} + (Mg-\square Mg)W_{\square Mg} + (Al-\square Al)W_{\square Al} + (Fe-\square Fe)W_{\square Fe}$$

$$RT\ln\gamma_{Mg-Am} = (Mg - MgAl)W_{AlMg} + (Fe - FeAl)W_{AlFe} - \square MgW_{\square Mg} + (\square - \square Al)W_{\square Al} - \square FeW_{\square Fe}$$

where

Mg, Al, Fe and $\square$ are molar fractions on M1.

INPUT DATA

Table 3 lists the experimental input data as well as the corresponding equilibria used to derive the chlorite endmember and solution thermodynamic properties. The natural input data are listed in the app.

Experimental Constraints

The first data available from the literature are analyses of chlorites equilibrated at fixed P-T conditions within a given mineral assemblage (Baker and Holland, 1996; Bryndzia and Scott, 1987). In such experiments, reversals were obtained by using different starting chlorite compositions, which should equilibrate with the same final composition. However, owing to the sluggish reaction rate close to equilibrium, differences in the final compositions are often observed. Experimental results were therefore interpreted as setting limits on the equilibrium composition at fixed P and T, and inequalities were derived from eq (3) through consideration of the direction from which equilibrium was approached.

Chlorites formed in the experiments of Baker and Holland (1996) are assumed to be devoid of vacancies (crystallization $T > 750°C$, see fig. 2), and the uncertainty on the compositions reported by the authors is fixed at XChl $\pm$ 0.035 on the basis of the scatter in the measured c parameter reported in their figure 4.

Chlorites crystallizing in the experiments of Bryndzia and Scott (1987) are also assumed to be devoid of vacancies, and all iron is assumed to be divalent. Moreover, Bryndzia and Scott (1987) reported that kyanite was corroded in the 6 kb pressure runs, strongly suggesting reaction of this phase. For this reason, the 6 kb results are interpreted in terms of Ky-free Chl-Qtz-Mt-H_2O-O_2 equilibrium reversals (equilibrium 12 in table 3).

Other types of experimental data used are P-T reversals of equilibria involving chlorite of known (Massonne, 1989) or unknown final composition (Staudigel and Schreyer, 1977; Chopin and Schreyer, 1983). For reasons of consistency, chlorite compositions estimated from cell parameter data are re-evaluated here using the new XRD-composition calibration obtained by Baker and Holland (1996). On the basis of the trends depicted in figure 2, the unknown amount of vacancy (not assessable from XRD) is estimated to be less than 0.1 a.p.f.u. In the case of the experiments of Chopin and Schreyer (1983) conducted at $T < 550$ °C (Car-Chl-Qtz-Ky-H_2O), the amount of vacancy is estimated to be less than 0.2 a.p.f.u., and it is estimated to be less than 0.1 a.p.f.u. for chlorite involved in the Cld-Chl-Ky-Co equilibrium ($550 < T < 700°C$).

TABLE 3

Experimental constraints used for the derivation of the endmembers chlorite thermodynamic data, and nonideal solid solution parameters

Experimental data	Bracketed equilibria or equilibrium assemblage	Assumed uncertainties	End-members chlorite equilibria		constrained parameters
		$MgO\text{-}Al_2O_3\text{-}SiO_2\text{-}H_2O$			
Baker and Holland (1996)	Chl + Opx + Fo + H_2O	$\pm$ (1% + 3°C); $\pm$ 500 bars Xchl $\pm$ 0.05	2Clin =2Fo + 2Opx +Am + H_2O	(1)	H°f & S° Am, W_{AlMg}(P,T)
	Chl + Sp + Co + H_2O		3Am = 2Sp + Co + 2Clin + 4H_2O	(2)	
Massonne (1989)	Chl + Qtz = Tc + Ky + H_2O	$\pm$ (1% + 3°C); $\pm$ 500 bars Xchl $\pm$ 0.05			W_{AlMg}(P,T)
Chopin and Schreyer (1983)	Car + Qtz = Chl + Ky + H_2O	$\pm$ (1% + 3°C); $\pm$ 500 bars	10Car + 3Am = 6Sud + 2Clin +2Ky	(3)	H°fAm, W_{AlMg}(P,T)
			3Sud + 2Clin = 7Qtz + 4Am + 4H_2O	(4)	
			14Ky + 4Clin+20H_2O = 8Sud + Am	(5)	
	Car + Dsp = Chl + Ky + H_2O	$\pm$ (1% + 3°C); $\pm$ 500 bars	8Clin + 28Dsp = 9Am + 2Sud + 2H_2O	(6)	H°fAm, W_{AlMg}(P,T)
			7Car + 2Am + 2H_2O = 5Sud + Clin	(7)	
			14Ky + 4Clin + 20H_2O = 8Sud + Am	(5)	
	Cld = Chl + Ky + Co + H_2O		8Clin + 14Co +12H_2O = 9Am + 2Sud	(8)	H°f,& S°Mg-ctd, W_{AlMg}(P,T)
		$\pm$ (1% + 3°C); $\pm$ 500 bars	14Ky + 4Clin+20H_2O = 8Sud + Am	(5)	
	Cld = Prp + Co + H_2O		Clin + 7Cld + 5H_2O = 2Sud +2Am	(9)	
					H°f,& S°Mg-ctd
Vidal and others. (1992)	Car = Sud + Qtz	$\pm$ (1% + 3°C); $\pm$ 500 bars	2 Car = Sud + Qtz	(10)	H°f & S° Sud
Staudigel and Schreyer (1977)	Chl = Opx + Fo + Sp + H_2O	$\pm$ (1% + 3°C); $\pm$ 500 bars	2Clin =2Fo + 2Opx +Am + H_2O	(1)	W_{AlMg}(P,T)
Jenkins and Chernosky (1986)			Am + Fo = Sp + Clin	(11)	
		$FeO\text{-}MgO\text{-}Al_2O_3\text{-}SiO_2\text{-}H_2O$			
Bryndzia and Scott (1987)	Chl+Mt + Qtz + H_2O + O_2 +Sill or Ky $\pm$ Tc	$\pm$ 10 °C ; $\pm$ 200 bars buffered fO_2 $\pm$ 0.5	4Clin + 6Dph + 5O_2 = 5Am + 10 Mt + 20Qtz + 20 H_2O	(12)	H°f Daph, W_{AlFe}(P,T)
Saccocia and Seyfried (1994)	Chl + Ab+Pg +Qtz + 3.2wt% NaCl aqueous fluid	$\pm$ 10 °C; Log(aFe^{2+}/aMg^{2+}) $\pm$ 0.2	20Fe^{2+} + 6Ab + 2Qtz + 5Am + 2H_2O = 4Daph + 6Pg + 20 Mg^{2+}	(13)	H°f Daph, W_{AlFe}(P,T)
			5Fe^{2+} + Clin = 5Mg^{2+} + Daph	(14)	

The third type of experimental constraints are solubility equilibria investigated by Saccocia and Seyfried (1994) for the assemblage Chl-Ab-Pg-Qtz in 3.2 wt percent NaCl fluids as a function of chlorite composition from 300° to 400°C, 500 bars. Sverjensky and others (1991) claimed that a –1626 cal/mol correction to the $\Delta G°f$ and $\Delta H°f$ of Na-silicate in the Berman (1988) data base is required to obtain consistency with the Ab-Pg-Qtz solubility data of Montoya and Hemley (1975). However, the magnitude of this correction is uncertain, and Saccocia and Seyfried (1994) proposed a –817 cal/mol adjustment. In view of these remaining uncertainties, Saccocia and Seyfried (1994) solubility data were used to constrain the aMg^{2+}/aFe^{2+} dependency as a function of chlorite composition and temperature of the Na^{+}-free equilibria only. Eqs (13) and (14) (table 3) were used for the "High-Mg chamosite" chlorite composition whereas equilibrium (14) was used only for the "Low-Fe clinochlore" composition. In effect, the amount of amesite component in "Low-Fe clinochlore" is too small to calculate a reliable Mg-amesite activity.

Natural data

About 200 analyses of chlorite involved in various parageneses were used as natural constraints. The on-site molar fractions of atoms (see table 1 for the calculation procedure) are listed in the app., but complete analyses are available from the authors upon request. Part of the natural data listed in the appendix comes from the literature, and when samples were available, new analyses were performed. These data were selected:

1. for the mineralogical assemblages or geological context that allows independent P-T estimates (listed in app.).
2. for the textural and chemical evidence of equilibrium among the relevant minerals. In particular, literature data were selected for the criteria used to distinguish "primary" from "secondary" chlorites. Classical micro-structural criteria are generally sufficient to identify "peak-temperature" from "retrograde" chlorites (Vidal and others, 1999), and when different chlorite generations appeared to coexist in the same thin section, we used the analyses of the peak temperature assemblages, as explicitly described by the authors. The analyses from carpholite-bearing samples of Bousquet (1998) and Agard (1999) and from chloritoid-samples of Vidal and others (1999), as well as those performed in this study, are representative of a population of at least three analyses in the same part of the thin section. Analyzed chlorites and coexisting minerals are in contact and do not exhibit reaction features. If mineral zoning was evidenced, we considered the rim analyses only.
3. in order to cover a wide range of P-T conditions (from diagenetic environment to 600°C, 2-25 kb).
4. for their range in mineralogy. We considered only natural examples in which quartz was present, in order to constrain the thermodynamic model so that the Chl + Qtz assemblage could be used later as a temperature indicator (based on the location of the temperature-dependent equilibrium (4), table 3).

Of the ~300 analyses initially collected, 10 percent were not used because of the insufficient level of confidence concerning the P, T estimates. We then rejected EMPA analyses showing an oxygen summation lower than 84 wt percent or higher than 91 wt percent as well as those showing more than 0.5 wt percent ($Na_2O + K_2O + CaO$). The remaining analyses were screened using the constraints (1) and (2) mentioned above.

CALCULATION PROCEDURE

The endmember standard state properties and the Margules parameters were calculated for fixed volumes, Cp(T) and V(P,T) functions (table 2). Linear programming (Berman and others, 1986) was used to solve inequalities derived from eq (1) for

each set of constraints through consideration of the direction from which equilibrium was approached in experiments and consideration of the P, T, and mineral composition uncertainties for natural data (McMullin and others, 1991). Since the input constraints are of different nature and have different levels of reliability, the unknown parameters were calculated step-by-step, as indicated below. This step-by-step calculation insures that maximal weight is put on the first set of constraints with the highest level of reliability and minimal weight on the last set of data. In other words, the thermodynamic data were calculated to be compatible with all individual constraints of the first set of data (experimental phase equilibria in MASH constraining the Mg-amesite properties and W_{AlMg}) and kept unchanged for the calculation of the other unknowns.

Mg-amesite Standard State Properties and WAlMg (P,T)

The Mg-amesite properties are directly tied to those of clinochlore used as input data. The clinochlore entropy from Berman (1988) is 25J/mol/K higher than the value predicted with Holland's (1989) method (configuration entropy = 11.52 J/mol/K). Therefore, the Mg-amesite third-law entropy ($S^{\circ}_{Mg\text{-}Am}$) is also expected to be higher than the value predicted with the Holland (1989) algorithm. It is constrained to lie between 385 (predicted value) and 410 J/mol/K (predicted value + 25 J/mol/K). The formation enthalpy of Mg-amesite ($H^{\circ}f_{Mg\text{-}Am}$) is constrained to be in the range of values predicted by Vieillard (1994). The W_{AlMg} Margules interaction energy is also constrained to lie within a specific range of values (5-30 kJ/mol) consistent with the W_{AlMg} = 21.431 kJ/mol calculated by Mäder and others (1994) for the M2 site of hornblendes (similar in sign and magnitude to values found by Aranovitch (1991) for orthopyroxene and Berman and others (1995) for clinopyroxene).

Initially $S^{\circ}_{Mg\text{-}Am}$ and $H^{\circ}f_{Mg\text{-}Am}$ were calculated with constant W_{AlMg} from the Baker and Holland (1996) P-T-X data (fig. 3A and B), which are the most constraining experimental data available from the literature. Following this, the P and T dependency of W_{AlMg} is calculated (for the H°f and S° determined above) in order to fit the Massonne (1989) P-T-X data obtained at lower temperatures and over a wider range of pressure conditions, as well as to fit reversals of Staudigel and Schreyer (1977) and Jenkins and Chernosky (1986) (see figs. 4 and 5).

Sudoite, Mg-carpholite, and Chloritoid Standard State Properties

Although they were not used in the above calculations, the Mg-carpholite thermodynamic data derived by Vidal and others (1992) are compatible with the Mg-amesite and W_{AlMg} data derived above. Indeed, both equilibria Car + Qtz = Chl + Ky + H_2O (fig. 4) and Car + Dsp = Chl + Ky + H_2O calculated with the Mg-amesite data obtained above lie within the brackets of Chopin and Schreyer (1983). Therefore, we also used the Mg-sudoite thermodynamic data from Vidal and others (1992), which are compatible with the Mg-carpholite data and the reversal of the equilibrium (10) (table 3).

Since a large part of the natural chlorite used in the following occur in Chl-Cld-Qtz assemblages, thermodynamic data for Mg-chloritoid (not included in the TWEEQ dataset) compatible with the clinochlore, Mg-amesite, and W_{AlMg} data are required. The Mg-chloritoid properties were calculated from the bracketing of the equilibria Mg-chloritoid = chlorite + corundum + kyanite + H_2O (fig. 6) and Mg-chloritoid = pyrope + corundum + H_2O (Chopin and Schreyer, 1983) with a $S^{\circ}_{Mg\text{-}Cld}$ fixed at 135 ± 5 J/mol/K. Using the Fe-Cld data from Vidal and others (1994), this is equivalent to fixing the 298K, 1 bar FeMg-1 exchange entropy to –26.7 J/K/atom (Spear and Cheney, 1989).

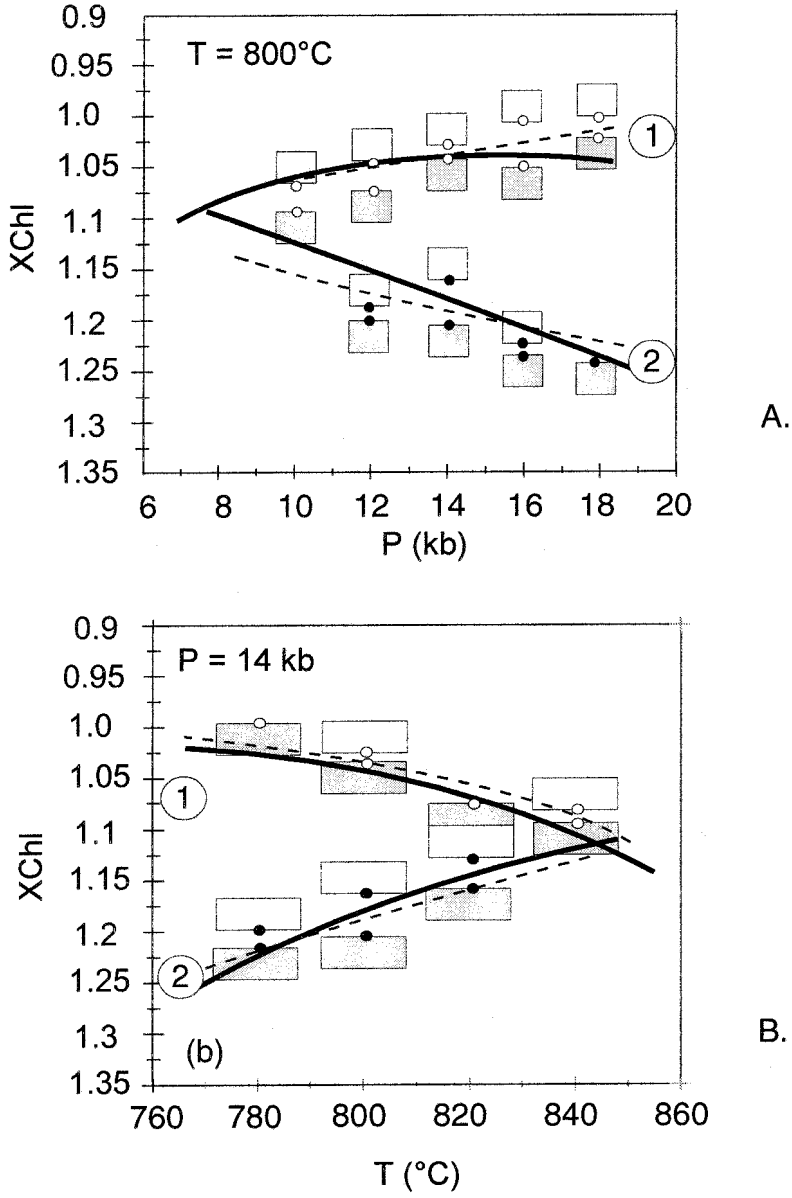

Fig. 3. Composition of chlorite (XChl = $Al^{IV}/2$) from reversal experiments of Baker and Holland (1996) for chlorite + orthopyroxene + forsterite (1) and chlorite + spinel + corundum (2). The circles show the experimental P-T conditions, and the boxes indicate the XChl, T, or P uncertainties assumed in the present study (see text). Dashed lines show the location of equilibria calculated with the chlorite solution model of Holland and others (1998), and solid lines the location of equilibria 2Clin =2Fo + 2Opx + Mg-Am + H_2O (1) and 3Mg-Am = 2Sp + Co + 2Clin + $4H_2O$ (2) using the chlorite thermodynamic data and solution model proposed in the present study.

Daphnite Standard State Properties and $W_{AlFe}(P,T)$

The daphnite entropy was constrained to lie within 568.7 ± 10 J/mol/K, corresponding to $S^\circ_{Daph} = S^\circ Clin - 5 \times S^\circ_{FeMg\text{-}1}$, with $S^\circ_{FeMg\text{-}1} = -26.7 \pm$ J/K/atom (Spear and

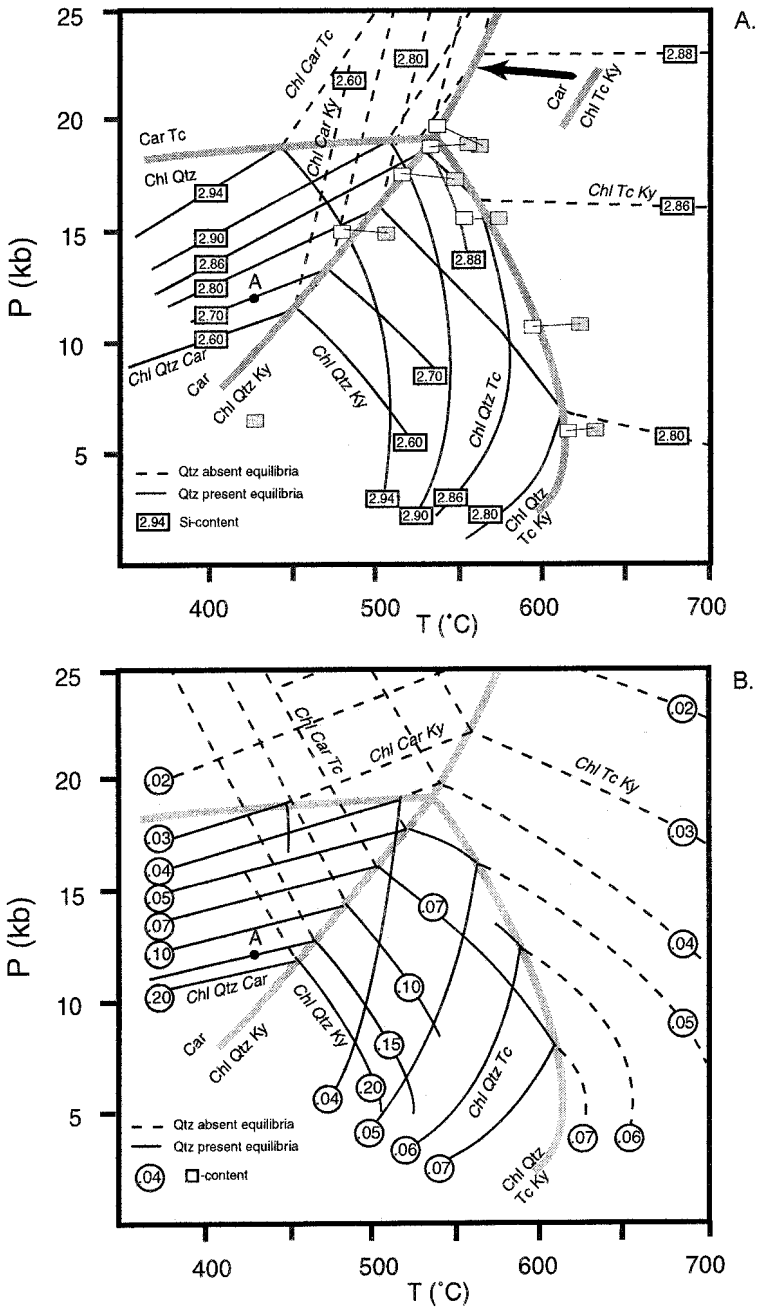

Fig. 4. Calculated chlorite composition in the MgO-Al_2O_3-SiO_2-H_2O system in presence of carpholite (Car), talc (Tc), kyanite (Ky), and quartz (Qtz). The thin lines show the equilibrium conditions for chlorites with (A) an iso-Si content (but variable □ and Al contents) or (B) iso □-content (but variable Si and Al contents) involved in the divariant assemblages. The composition of chlorite can be calculated by combining (A) and (B). For example, the composition of chlorite coexisting with carpholite and quartz at point A is $Si_{2.7}Al_{2.6}Mg_{4.25}\square_{0.15}O_{10}(OH)_8$. At this point, the equilibria $3Sud + 2Clin = 7Qtz + 4Am + 4H_2O$, $Clin + 3Car = 5Qtz + 2Am + 2H_2O$, $5Sud + Clin = 7Car + 2Am + 2H_2O$, and $2Car = Sud + Qtz$ intersect. The thick gray lines show the location of the univariant equilibria. The boxes in (A) show the experimental reversal from Massonne (1989) and Chopin and Schreyer (1983).

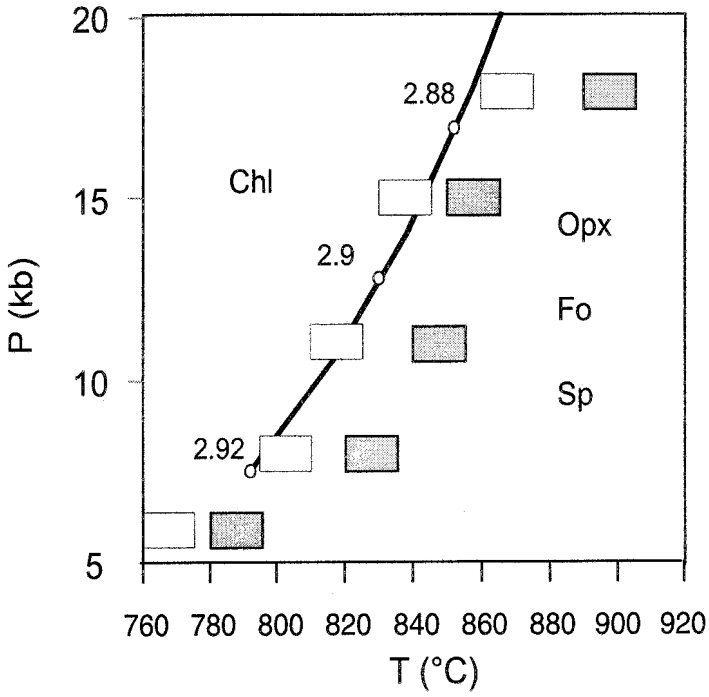

Fig. 5. Experimental bracketing of the equilibrium chlorite = orthopyroxene + forsteite + spinel + H_2O after Staudigel and Schreyer (1977) and Jenkins and Chernosky (1986). The calculated location of this equilibria (assuming □ = 0) is shown by the curve, and the numbers indicate the calculated Si-content in chlorite (a.p.f.u. with a 14 oxygen basis).

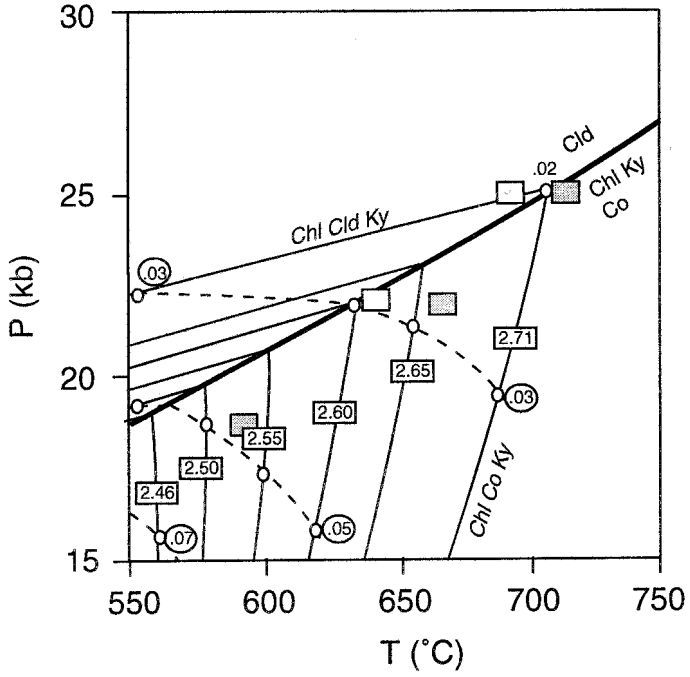

Fig. 6. Experimental bracketing of the equilibrium chloritoid = chlorite + kyanite + corundum + H_2O after Chopin and Schreyer (1983). Thick line: calculated location of this equilibria. Thin lines: Si- and □- (discontinuous lines) isopleths in the divariant fields.

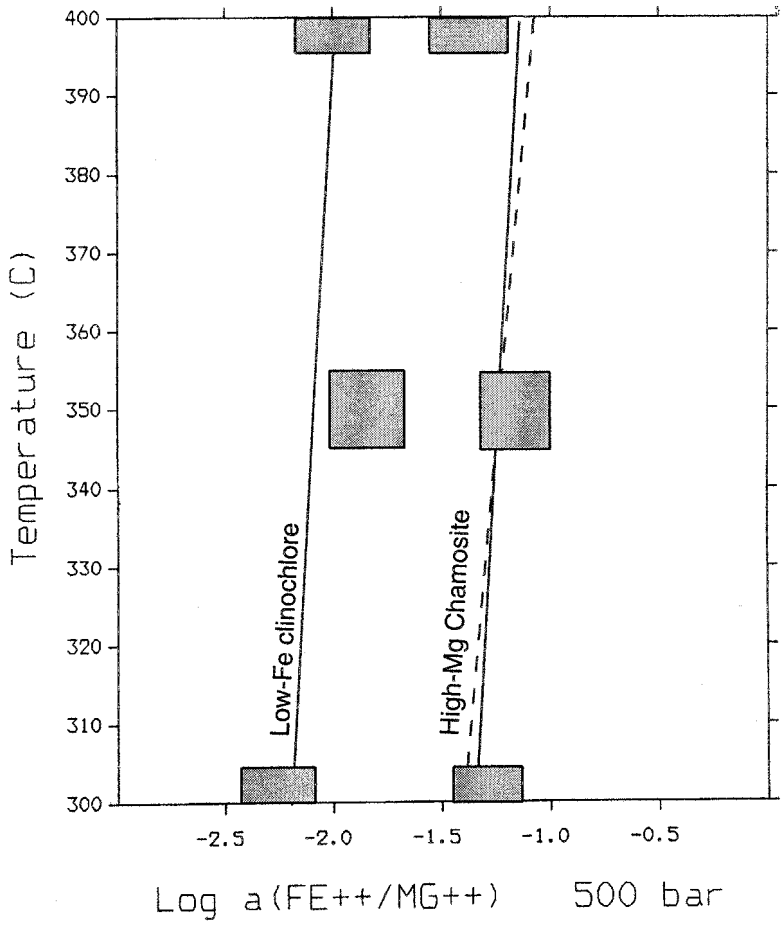

Fig. 7. The aFe^{2+}/aMg^{2+} ratio for the assemblage Chl-Ab-Pg-Qtz in 3.2 wt percent NaCl fluids as a function of temperature for two chlorite compositions (Saccocia and Seyfried, 1994). The boxes correspond to the solubility measurements expanded to account for experimental uncertainties and uncertainties coming from the speciation model adopted by the authors. Lines are the calculated ratios using the chlorite data listed in table 2 and thermodynamic data for aqueous species from the TWEEQ data base. Solid lines : $5Fe^{2+}$ + Clin = $5Mg^{2+}$ + Daph; dashed line : $20Fe^{2+}$ + 6Ab + 2Qtz + 5Mg-Am + $2H_2O$ = 4Daph + 6Pg + 20 Mg^{2+}

Cheney, 1989). W_{AlFe} was constrained to lie between −30 and −5 kJ/mol to be consistent with the W_{AlFe} = −15.5 kJ/mol calculated by Mäder and others (1994) for the M2 site of hornblendes (similar in sign and magnitude to the values found by Aranovitch (1991) for orthopyroxene and Berman and others (1995) for clinopyroxene). The daphnite properties and W_{AlFe} parameter were calculated to locate the aFe^{2+}/aMg^{2+} *versus* temperature equilibria (13) and (14) (table 3) within the experimental constraints of Saccocia and Seyfried (1994) (fig. 7). The experimental aFe^{2+}/aMg^{2+} values were computed from the Fe and Mg solubility data and fluid speciation model of Saccocia and Seyfried (1994).

Attempts to calculate daphnite thermodynamic data and W_{AlFe} compatible with all the experimental results reported by Bryndzia and Scott (1987) (fig. 8) were impossible, because the compositions obtained for different runs conducted at the same P-T-fO_2 conditions with the same starting mixtures are in some cases very different. In

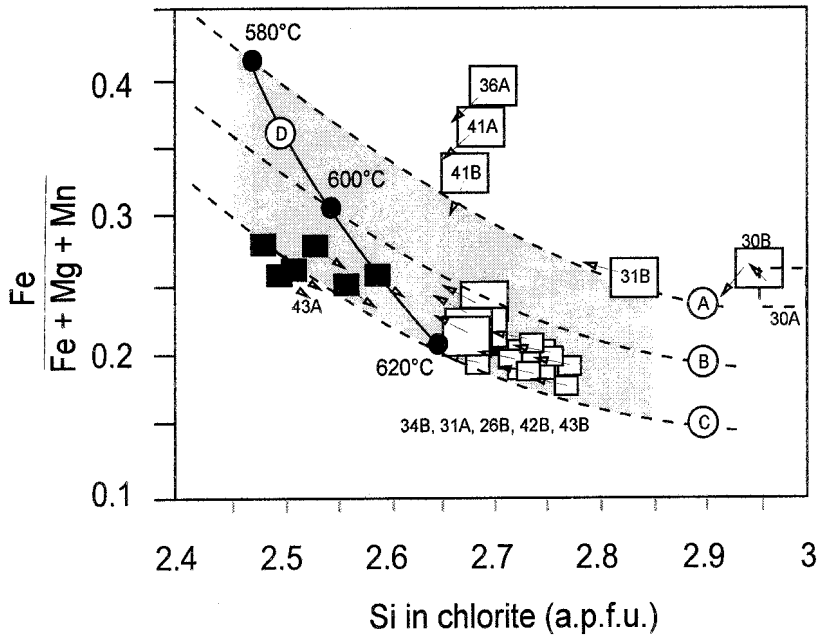

Fig. 8. Final chlorite compositions from the Bryndzia and Scott (1987) sulfidation and oxidation experiments. Small squares are from experiments 43A and B. Arrows indicate the direction in which the chlorite compositions evolved from the starting compositions. Dashed lines : calculated composition of chlorite in equilibrium with Mt + Qtz + O_2 + H_2O at 6 kb, 580°C (A), 600°C (B), and 620°C (C). Gray area : composition of chlorite in equilibrium with Mt + Qtz + O_2 + H_2O at 600°C, 6 kb assuming a logfO_2 (buffered) ± 0.5 uncertainty. Continuous line (D) : composition of chlorite in equilibrium with Ky + Mt + Qtz + O_2 + H_2O at 6 kb, 580° to 620°C (solid circles).

particular, large Si/Al differences are observed among chlorites equilibrated with the same assemblage at the same P-T-fO_2-fS_2 conditions (runs 30B, 31B, and 34B). This suggests that equilibrium was not achieved in all experiments. Incomplete equilibration is also indicated for most final compositions in runs 43A and B. However, since most of the final chlorites in the 600°C-6 kb runs (34B, 31A, 26B, 42B, 43B) show $2.65 < Si < 2.75$ and $0.15 < XFe < 0.25$, the Chl-Qtz-Mt- H_2O-O_2 equilibrium is believed to be closely approached for these compositions. We used the direction in which the chlorite composition evolves from the starting composition (depicted by the arrows on fig. 8) to write inequalities derived from eq 3.

The daphnite data and the P and T dependency of W_{AlFe} also rely on the composition of natural chlorites with $\square < 0.025$ associated with chloritoid and quartz for which reliable P-T conditions of formation are available. The thermodynamic properties were constrained in order to locate the (Daph + Clin + Mg-Am)$_{in\ chlorite}$ + (Fe-, Mg-Cld) + Qtz + H_2O invariant point at the temperature equal to that estimated with the Chl-Cld exchange thermometer from Vidal and others (1999) (± 30°C) and pressure conditions in agreement with those determined originally (± 30 percent).

Chlorite-garnet natural data were not used as constraints, because textural evidence for equilibrium between chlorite and garnet is often equivocal. Moreover, garnets are generally zoned, and the determination of chlorite-garnet equilibrium compositions is uncertain. Another source of uncertainty comes from the generally low Mg-contents ($XMg < 0.1$) of garnet and therefore the significant influence of small analytical uncertainties on the magnitude of the chlorite-garnet Fe-Mg partitioning

coefficient. However, selected chlorite-garnet natural data were used to check the consistency of the properties derived above with the garnet and biotite solid solution properties from Berman (1990) and McMullin and others (1991), respectively.

$W\square_{Mg}$, $W\square_{Al}$, and $W\square_{Fe}$ Margules Parameters

The difference $W\square_{Mg} - W\square_{Al}$ was estimated so that sudoite-trioctahedral chlorite unmixing occurs in MASH at T < 500°C as is suggested by the co-stability of clinochlore and sudoite in experiments (Fransolet and Schreyer, 1988; Vidal and others, 1992) and in nature (Franceschelli and others, 1989; Theye and others, 1992; Zhou and Phillips, 1994; Oberhänsli and others, 2000). Because of the lack of experimental constraints on the extent of the DT substitution with pressure and temperature, the $W\square_{Al}$, $W\square_{Mg}$, and $W\square_{Fe}$ functions were estimated from natural data obtained at T < 500°C. They were derived to obtain realistic temperature conditions for the equilibrium 2 Clin + 3 Mg-Sud = 4 Mg-Am + 7 Qtz + 4 H_2O (4), that is the chlorite + quartz paragenesis, assuming $aH_2O = 1$. As shown in figure 2, the amount of (Mg,Fe)-amesite and -sudoite components are very low in the 275° to 350°C range at low pressure and above 500°C at high pressure. For these chlorite compositions, analytical uncertainties have a major impact on the activity of Mg-amesite and -sudoite and therefore on the equilibrium constant of (4). For this reason, we decided to use only those analyses in which X(Mg,Fe)-Am and X(Mg,Fe)-Sud > 0.045 (49 analyses of an initial set of 68 low-T, low-P samples, 69 of 80 Chl-Cld analyses). A first estimate of $W\square_{Al}$, $W\square_{Mg}$, and $W\square_{Fe}$ was obtained from the low-T and low-P (< 1 kb) samples. The final $W\square_{Al}$(P,T), $W\square_{Mg}$(P,T), and $W\square_{Fe}$(P,T) functions were adjusted to fit the following natural data:

1. fifty low-temperature (< 450°C) carpholite-chlorite-quartz data (Bousquet, 1998 and Agard, 1999). In the absence of thermodynamic data for Fe-carpholite (no calorimetric or experimental data), the carpholite-chlorite-quartz equilibrium conditions were calculated using Mg endmembers only. They correspond to the point where the equilibria (4), (10), Clin + 3 Car = 5 Qtz + Mg-Am + 2 H_2O, and 5 Mg-Sud + Clin = 7 Car + 23 Mg-Am + 2 H_2O intersect.
2. sixty-nine chloritoid-chlorite-quartz data involving chlorite with $\square$ > 0.03 (app.). The equilibrium conditions for this paragenesis is realized at the intersection point of 14 equilibria (involving Daph, Clin, Mg-Am, Mg-Sud, Mg-, and Fe-Cld, Qtz, and H_2O). Ideally, the chlorite-chloritoid Fe-Mg exchange reaction:

$$\text{Daph} + 5\ \text{Mg-Cld} = \text{Clin} + 5\ \text{Fe-Cld} \qquad (15)$$

and equilibrium (4) intersect at this point (fig. 9A). In practice, however, the equilibrium constant for (4) is much more sensitive to small compositional changes than the equilibrium constant of (15). Since the slopes of these two temperature-dependent reactions are close, small variations in the chlorite composition lead to large variations in the P-T location of the point where (4) and (15) intersect. In particular, small variations in the amount of vacancies lead to an important temperature shift of (4) but not of (15). For this reason, $W\square_{Al}$(P,T), $W\square_{Mg}$(P,T), and $W\square_{Fe}$(P,T) functions were primarily constrained in order to locate the invariant point involving Clin, Am, Daph, Fe- and Mg-Cld, Qtz, H_2O at a temperature equal to that estimated with the Chl-Cld exchange thermometer from Vidal and others (1999) (± 30°C uncertainty). They were then adjusted to minimize the difference between the Fe-Mg exchange reaction and equilibrium (4) (fig. 9B and C).
3. four Sudoite-chloritoid-quartz data. We attempted to use the conditions of the Sud-Cld-Qtz equilibrium as an additional constraint for the $W\square_{Al}$(P,T),

$W\square_{Mg}$(P,T), and $W\square_{Fe}$(P,T) calibration. However, in most cases, the sudoite analyses available in the literature show a Si content > 3 a.p.f.u., whereas our activity model pertains only for chlorites with a Si content less than 3 a. p.f.u.. The few Sud-Cld analyses listed in the appendix were obtained from samples from the Lycian nappes (Oberhänsli, unpublished data) and from the Peloponnese (Trotet, unpublished data).

RESULTS AND DISCUSSION

The calculated thermodynamic data and the chlorite solution parameters are listed in table 2. It is emphasized that the thermodynamic properties derived in this study are model-dependent and therefore are only compatible with the thermodynamic data used for their calculation as well as the atom site partition calculated as reported in table 1.

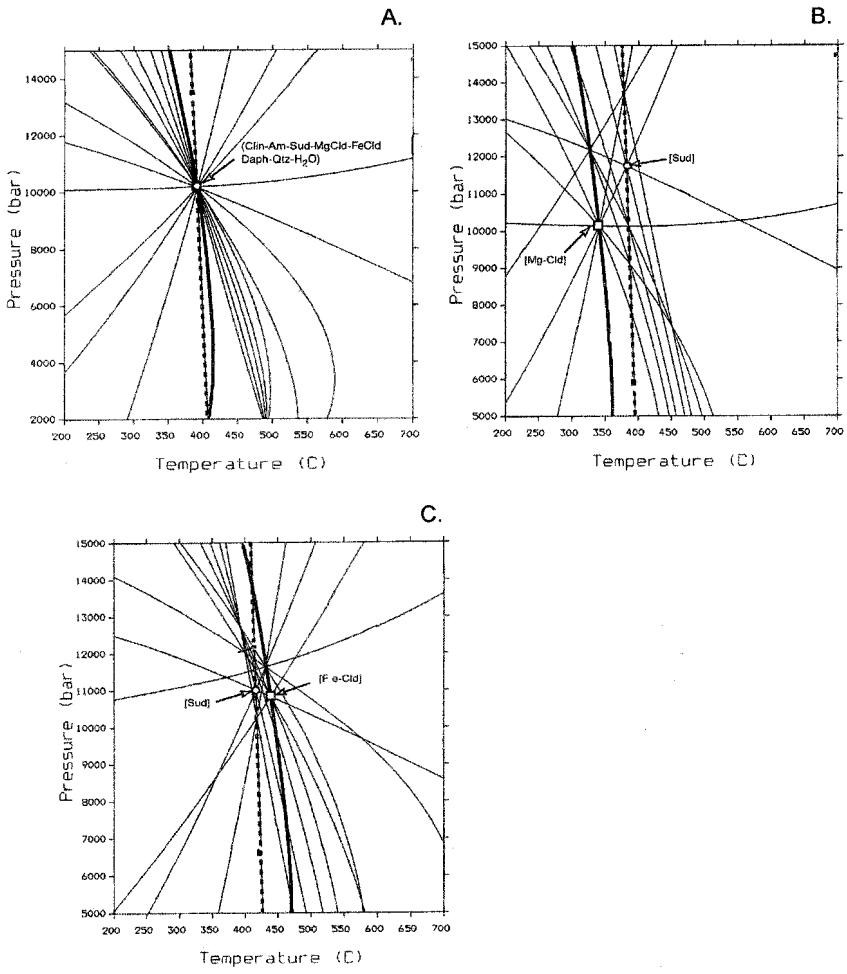

Fig. 9. Examples of multivariant equilibria calculation for the Chl-Cld-Qtz paragenesis. (A) Chl14-Cld23 from the Lycian nappes (Oberhänsli, table 4); (B) and (C): Chl68-Cld and Chl65-Cld respectively, from the Valaisan Zone (Vidal and others, 1999; table 4). Thick curves: 2Clin + 3Mg-Sud = 7Qtz + 4Mg-Am + H_2O (dashed) and 5Mg-Cld + Daph = Clin + 5Fe-Cld (solid). Circle : Sudoite-absent invariant (column "II"in table 4). Square : Mg-Cld absent invariant when $T_{(4)} < T_{\text{Clin-Daph-Fe,Mg-Cld}}$ or Fe-Cld absent invariant when $T_{(4)} > T_{\text{Clin-Daph-Fe,Mg-Cld}}$ (see text for details).

As shown in figures 3 to 8, these data allow one to fit the experimental results obtained in the MASH and FMASH system listed in table 3 in the limit of the uncertainties and the assumptions made on the chlorite composition discussed above.

MgO-Al_2O_3-SiO_2-H_2O Experimental System

Using the thermodynamic data listed in table 2, we have recalculated the composition of chlorite involved in divariant assemblages at low temperature. For reasons of clarity, results are reported on separate parts of figure 4 (A shows the chlorite Si-content and B the □-content), but the Si-and □-content were calculated simultaneously. For example, equilibria (4), (7), (10) and Clin + 3 Car = 5 Qtz + 2 Mg-Am + 2 H_2O involving a chlorite of $Si_{2.7}Al_{2.6}Mg_{4.25}\square_{0.15}O_{10}(OH)_8$ composition intersect at point A, located at 431°C, 11.9 kb on figure 4A and B. The Si-content isopleths reported on figure 4A correspond to the lines going through all the intersection points involving a chlorite of constant Si- but variable Al-, Mg-, and □-contents, whereas the □-isopleths are lines of iso □-content but variable Si, Al-, and Mg-contents.

Our results indicate that the Si- and □-contents have opposite variations with changing P-T conditions. In the chlorite-carpholite-quartz stability field, the amount of vacancy is calculated to increase rapidly with decreasing pressure, and it is predicted to be more than 0.2 a.p.f.u. below 10 kb. Although this amount may seem large, it does correspond to amounts inferred from natural Fe-Mg chlorites associated with carpholite (Bousquet, 1998; Agard, 1999, see app.). The predicted low Si-contents at these conditions also correspond to what is observed in nature.

At higher temperature, a slight increase in the content of vacancies and a decrease in Si with increasing temperature are predicted for the Chl-Qtz-Tc paragenesis, whereas the opposite is predicted for the Chl-Qtz-Ky paragenesis. It is noteworthy that below 500°C, the composition of chlorite coexisting with Tc and Qtz (in the absence of Ky) should be close to that of pure clinochlore. The chlorite compositions calculated for this assemblage are in agreement with those observed in nature by Moine and others (1982) ($2.86 < Si < 3$; $0.01 < \square < 0.05$ for $0.88 < XMg < 0.95$ at ~475°C, 1 kb) and Schreyer and others (1982) (Si = 3.04, □ = 0.015 for XMg = 0.99 at ~400°C).

At still higher temperature, the amount of vacancy in chlorite is low, and it has no influence on the location of the equilibria studied by Baker and Holland (1996), Staudigel and Schreyer (1977), Jenkins and Chernosky (1986), and Bryndzia and Scott (1987). This justifies *a posteriori* the assumptions made for the calculation of the amesite thermodynamic data and the W_{AlMg} interaction parameter, that is that chlorites are devoid of vacancies in these experiments.

MgO-FeO-Al_2O_3-SiO_2-H_2O experimental system

We have reported on figure 7 the predicted and experimental aFe^{2+}/aMg^{2+} ratio in 3.2 wt percent NaCl solution equilibrated with the two chlorite compositions used by Saccocia and Seyfried (1994). The good agreement between predicted and experimental values indicates that the relative thermodynamic properties of daphnite, Mg-amesite, and clinochlore as well as the mixing properties between these endmembers are consistent with the solubility data. In particular, the aqueous Fe/Mg concentration ratio of NaCl solutions coexisting with chlorite is predicted to increase with temperature and mole fraction of daphnite, which is consistent with the experimental results.

Figure 8 shows the final chlorite compositions analyzed by Bryndzia and Scott (1987) and the compositions calculated for chlorite in equilibrium at 6 kb with the Mt-Qtz-O_2-H_2O (dashed lines for T =580°, 600°, and 620°C) and Ky-Mt-Qtz-O_2-H_2O (points) assemblages. Figure 8 also shows that our thermodynamic data are consistent with all the experimental results except run 30A and their associated uncertainties (T ± 10°C, P ± 200 bars, $\log fO_2$ (buffered) ± 0.5, Si(Chl) ± 0.05 a.p.f.u., XFe ± 0.025). Runs 41A, 36, and 30 lie outside the compositional area calculated for the

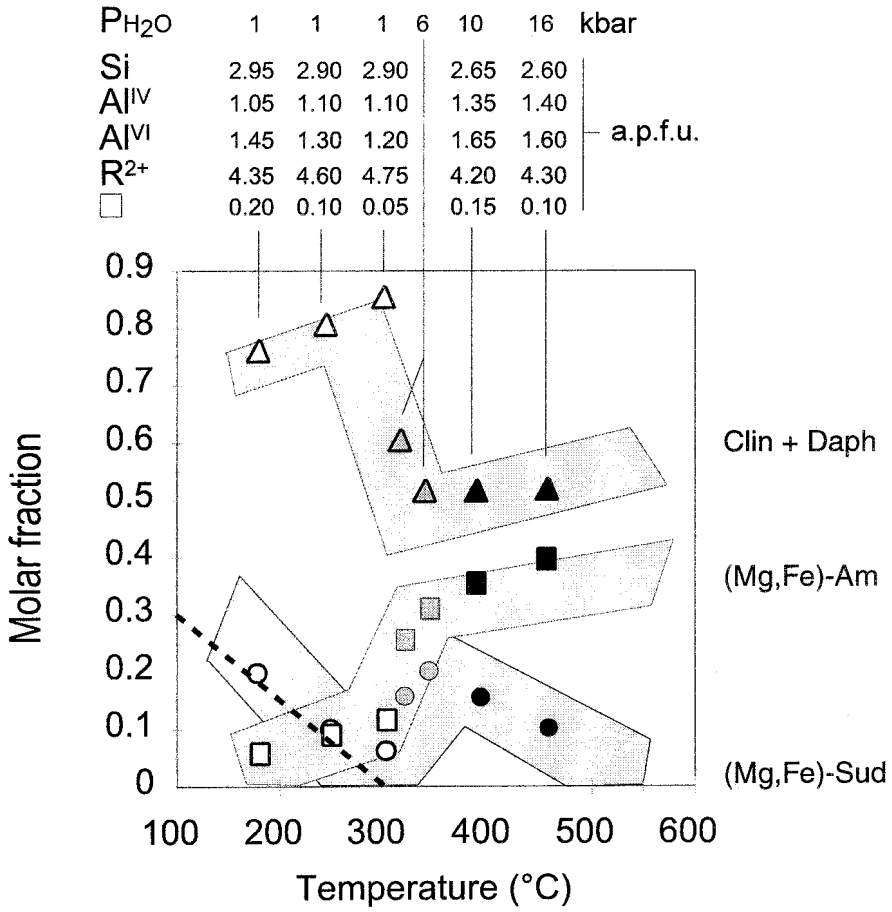

Fig. 10. Calculated molar fractions of (Fe,Mg)-sudoite (circles), -amesite (squares), and (clinochlore + daphnite) (triangles) in chlorites of fixed XMg = 0.5 equilibrated with quartz and H_2O (eq 4). Dashed line : empirical □ = f(T) relation proposed by Cathelineau and Nieva (1985).

Chl-Mt-Qtz-O_2-H_2O equilibrium (in gray on fig. 8), but the direction in which the chlorite composition evolves from the starting composition (indicated by the arrows) is compatible with the approach toward equilibrium, that is toward the calculated discontinuous lines and gray area.

Natural data

In the following, we compare the new P-T estimates obtained with the chlorite model presented above with the reference values for the calibrant samples (app.). Since the P-T calculation method is paragenesis-dependent, we discussed the reliability of our estimates for each set of calibrant samples independently. However, the first validity test consists of comparing the compositional trend predicted with the model for chlorite + quartz assemblages with that evidenced in figure 2. We have calculated the clinochlore + daphnite, (Fe,Mg)-amesite and -sudoite molar proportions in chlorites of fixed XMg = 0.5 for various temperature and pressure conditions. Results are reported on figure 10 with the corresponding chlorite structural formulae and equilibrium pressure conditions. They show that

the equilibrium compositions of chlorite associated with quartz and their evolution with changing temperature and pressure are in good agreement with those observed in nature. In particular, the solid-solution model accounts for the decrease in Si, Al^{VI}, and □ and the increase in Al^{IV} and (Fe + Mg) with increasing temperature and to the decrease of Si, (Fe + Mg) and increase of Al^{IV}, Al^{VI}, and □ with increasing pressure. The chlorite model is therefore at least qualitatively consistent with the observations of McDowell and Elders (1980), Cathelineau and Nieva (1985), Cathelineau (1988), Hillier and Velde (1991), DeCaritat and others (1993), and Leoni and others (1998). It confirms that octahedral vacancies are a real feature at $T < \sim 300°C$, $P < 1$ kb which contributes to stabilize chlorite at low-T conditions. This indicates that octahedral vacancies should not be considered as an artifact resulting from incorrect normalization or contamination by other sheet silicates, as suggested by Jiang and others (1994).

A more detailed and quantitative discussion considering the additional role of XMg is done in the following by considering each set of data individually. The new P-T estimates obtained for each sample used in the calibration are listed in the app..

Chl-Cld-Qtz assemblages.—Three kinds of P-T estimates are reported in the app.. The first column lists the temperature location of equilibrium (4) at the pressure determined by the equilibrium Mg-Sud + Daph + Mg-Am = Fe-Cld + Clin + H_2O when $T_{(4)} < T_{(15)}$ or Mg-Am + Qtz = Mg-Cld + Clin + H_2O when $T_{(4)} > T_{(15)}$ (circles on fig. 9A and B). The second column lists the P-T conditions of the sudoite-absent invariant point where Mg-Am, Clin, Daph, Fe- and Mg-Cld, Qtz, and H_2O coexist (squares on fig. 9A, B, and C), and the third column gives the temperature estimated with the LnKd (= $(Fe/Mg)^{Cld}/(Fe/Mg)^{Chl}$) = f(T) equation from Vidal and others (1999).

The chlorite thermodynamic properties calculated above allow one to reproduce the original P-T estimates (column "IV" in app.) within their associated uncertainties. The sudoite-absent invariants (column "II") are located at pressures that are in reasonable agreement with the original estimates and temperatures consistent with those determined with the LnKd = f(T) equation from Vidal and others (1999) (fig. 11). The temperatures estimated from the chlorite + quartz equilibrium (4) (column "I" in table 4) are less reliable, but they are generally consistent with those obtained from the location of equilibrium (15) (12 out of the 69 samples show $T_{(4)} - T_{(15)} > \pm 50°C$.

Chl-Car-Qtz assemblages.—Temperatures calculated for these samples rely on the location of equilibrium (4) only. However, it is emphasized that in contrast to the low-P-T Cld-Chl-Qtz samples (Dauphinois zone, app.), chlorites associated with carpholite are generally larger in size, because higher pressure conditions favor the formation of larger grains. As a consequence, the risk of obtaining contaminated chlorite analyses in the Chl-Car-Qtz samples is lower, and the reliability of the temperature estimates should be better, although the temperature conditions are similar. This is confirmed by the reasonably low scatter of the calculated temperatures which are in good agreement with the original estimates (app. and fig. 12). The pressure conditions constrained by the intersections of (4) and 2Car = $Sud_{(in\ Chl)}$ + Qtz are also in good agreement with the previous estimates.

Low-T Chl-Qtz assemblages.—As expected, the temperatures calculated from the location of equilibrium (4) for the low-T samples are generally lower than for the Chl-Cld and Chl-Car samples. We have reported on figure 12 the calculated temperature against the reference values (measured borehole temperatures or independent estimates). In most cases, the calculated temperatures are in reasonable agreement (±50°C) with the reference values. Since the present-day borehole temperatures may not correspond to the paleo-geotherm at which chlorite crystal-

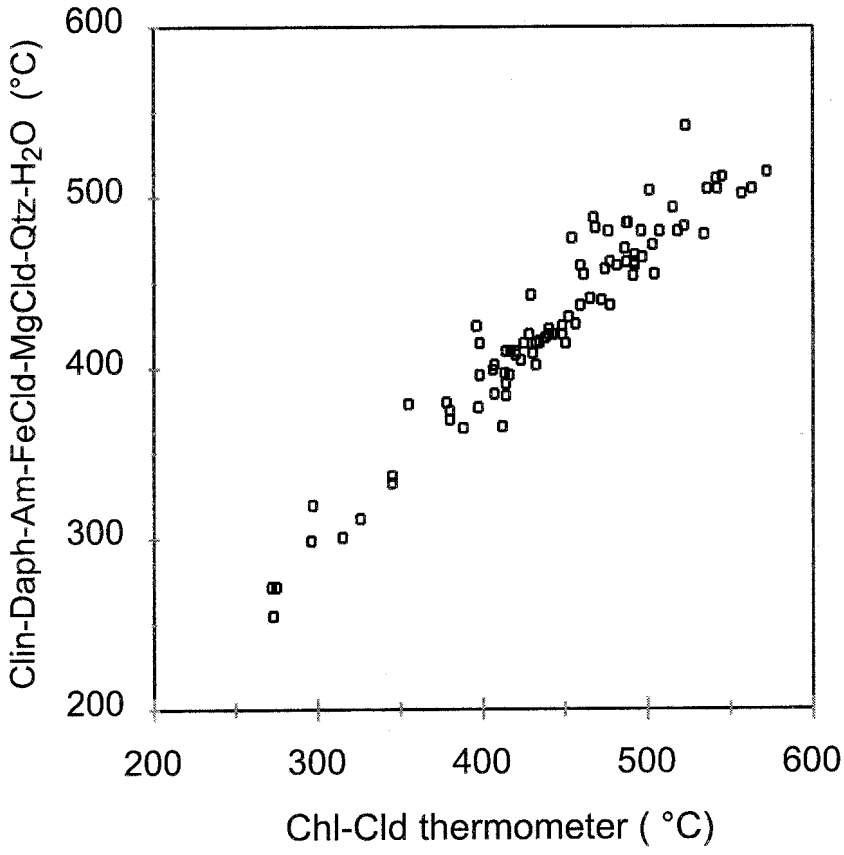

Fig. 11. Calculated equilibrium temperature for the Clin-Daph-Mg and FeCld-Qtz assemblages (circles on fig. 9, column "II" in table 4) versus temperature obtained for the same Chl-Cld pairs with the Fe-Mg Chl-Cld empirical thermometer from Vidal and others (1999) (column "III" in table 4).

lized (Hillier and Velde, 1991), a certain deviation between the calculated temperature and the reference temperature is possible. We have reported in the app. the temperatures calculated with the empirical thermometers of Cathelineau (1988) and Hillier and Velde (1991). The temperature ranges defined by these empirical thermometers and the reference temperature are depicted by horizontal bars in figure 10. Most of the temperatures determined from the location of equilibrium (4) lie within this range of temperature. They are overestimated by more than 50°C for 5 samples of the 49 listed in the app. (dashed line in fig. 12). There is no chemical argument to discard these 5 analyses. Therefore, a possible explanation for these overestimated temperatures may be the assumption that chlorite was equilibrated with a fluid with $aH_2O = 1$. Indeed, lowering the water activity leads to a shift of (4) to lower temperatures.

APPLICATION EXAMPLES

An independent test and application example of the chlorite properties consist of recalculating the P-T conditions of Gt-Chl bearing samples not involved in the calibration, for which reliable estimates are available. Two chlorite-garnet-quartz (± epidote ± biotite ± plagioclase) samples suites from the File Lake, Manitoba (Gordon

and others, 1991) and the Iberian massif (Arenas and others, 1995) were selected on the basis of their mineralogy which allow chlorite-independent P-T estimates, and for the detailed description of the textural relations and equilibrium criteria. The on-site atom partitioning calculated from the analyses are reported in table 4.

TABLE 4

Composition of natural minerals from Gordon and others (1991) (G91) and Arenas and others (1995) (A95). The molar fraction of atom per site is calculated as indicated in table 1

Chlorite-Garnet-Quartz ± Chloritoid, Plagioclase **CHL [Si Al]$_{T2}$ [Mg Fe Al □]$_{M1}$ [Mg Fe Al]$_{(M2+M3)}$** **GARN [Gros Prp Alm Sps]** **PLAG [Ca Na K]** **BIOT [Mg Fe Ti Al]$_M$ [K]$_A$ [OH]$_H$**	Sample	I T (°C)	 P (kb)	II T (°C)	III T (°C)	 P (kb)	IV	Original estimates T (°C)	 P (kb)	Reference
CHL .269 .729 .259 .282 .459 .000 .478 .521 .000	1001	561[1]	3(*)	491	540 ± 9.9	1.92 ± 0.28	3 IR, 14 Equ.	510-560	2-4	G91
GARN .037 .090 .820 .051		515[2]								
PLAG .251 .746 .028										
BIOT .359 .454 .032 .147 .948 1.00										
CHL .280 .718 .261 .285 .445 .009 .476 .519 .005	2025	564[1]	3(*)	490	541 ± 12.3	1.73 ± 0.43	3 IR, 14 Equ.			
GARN .036 .092 .839 .050		530[2]								
PLAG .242 .752 .006										
BIOT .326 .455 .030 .132 .829 1.00										
CHL .260 .737 .259 .262 .476 .003 .497 .501 .001	2038	550[1]	3(*)	518	549 ± 4.8	1.96 ± 0.38	3 IR, 14 Equ.			
GARN .041 .095 .831 .033		510[2]								
PLAG .301 .696 .0028										
BIOT .361 .425 .033 .147 .839 .972										
CHL .254 .741 .303 .237 .485 .000 .566 .442 .000	2040/2	573[1]	3.2(**)	502	559 ± 7.1	2.95 ± 0.52	4 IR, 29 Equ.			
GARN .063 .117 .726 .112		571[2]								
PLAG .449 .540 .0103										
BIOT .390 .394 .030 .135 .912 .974										
Iberian Massif										
CHL .333 .667 .338 .309 .333 .019 .516 .471 .010	1chl1/I	500[1]	12.4(**)	371	491.4 ± 7.3	12.33 ± 0.93	acz = 0.26	470-510	13.5-15.5	A95
GARN .211 .046 .654 .069	1gt1r/I						3 IR, 14 Equ.	(M1)		
CHL .335 .665 .353 .333 .330 .001 .512 .483 .001	2chl1/I	482[1]	12.1(**)	341	483 ± 0.8	12.17 ± 0.1	acz =0.25			
GARN .211 .040 .654 .088	2gr1r/I						3 IR, 14 Equ			
CHL .322 .670 .288 .354 .344 .014 .441 .541 .007	*3chl1*	*559[1]*	*7.4(**).*	*450*	*466 ± 56*	*13.04 ± 3.15*	acz = 0.19			
GARN .192 .045 .620 .124	*3gr1r/I*						3 IR, 14 Equ.			
CHL .328 .669 .308 .318 .346 .027 .477 .492 .013	4chl1/I	492[1]	10.6(**)	375	483 ± 6.4	10.68 ± 0.85	acz = 0.21			
GARN .191 .038 .593 .170	4gr1r/I						3 IR, 14 Equ			
CHL .289 .710 .314 .320 .421 .001 .499 .510 .001	4ch2/I	496[1]	8(**)	433	498 ± 1.6	7.98 ± 0.34	acz = 0.20			
GARN .161 .045 .610 .135	4gr3r/I						3 IR, 14 Equ			
CHL .301 .698 .315 .296 .412 .001 .517 .485 .001	1ch2/II	471[1]	11.5(**)	374	491 ± 11.9	12.32 ± 0.71	3 IR, 14 Equ	485-530	10-14	
GARN .099 .051 .684 .111	5gr1r/II							(M3)		
PLAG .032 .968 .00	5pl2									
CHL .312 .684 .343 .282 .374 .001 .540 .445 .001	2ch2/II	492[1]	11.8(**)	393	504 ± 6.8	12.22 ± 0.41	3 IR, 14 Equ			
GARN .090 .062 .671 .123	6gr1r/II									
PLAG .032 .968 .00	5pl2									
CHL .323 .674 .363 .293 .349 .001 .550 .443 .001	3ch2/II	493[1]	11.6(**)	387	504 ± 6.5	12.03 ± 0.39	3 IR, 14 Equ			
GARN .090 .062 .671 .123	6gr1r/II									
PLAG .032 .968 .00	5pl2									
CHL .267 .730 .255 .291 .475 .000 .469 .537 .000	7chl/III	548[1]	7.7(**)	458	535 ± 7	7.31 ± 0.41	4 IR, 29 Equ.	505-540	6.5-9	
GARN .1340 .0639 .7374 .0647	9gt1r/II	548[2]						(M4)		
PLAG .177 .812 .01	10pl1									
BIOT .343 .477 .020 .123 .980 1.00	9bt2/II									
CHL .327 .672 .317 .291 .343 .049 .505 .462 .024	11ch/III	560[1]	5.15(**)	450	551 ± 6.8	4.92 ± 0.65	4 IR, 29 Equ.			
GARN .1198 .0769 .7326 .0708	10gr1r/II	560[2]								
PLAG .268 .732 .00	11pl1									
BIOT .333 .437 .020 .150 .960 1.00	9bt1/II									

I: Gt-Chl (1) and Gt-Bt (2) exchange reactions at fixed (*) or calculated (**, Chl-Gt-Qtz-Bt or Ep invariant) pressure; II: Gt-Chl thermometer of Grambling (1990); III: TWEEQ computation of equilibria among chlorite, garnet, plagioclase and quartz and H_2O in the system CaO-MgO-FeO-K_2O-Al_2O_3-SiO_2-H_2O (1 σ uncertainties from INTERSX); IV: clinozoisite activities (acz), number of independent reactions (IR) and number of equilibria on which the results listed in III are based.

The equilibrium conditions were calculated using the INTERSX software (included in the TWEEQ package; Berman, 1991), using the solution model and mixing properties from Berman (1990) for garnet, McMullin and others (1991) for biotite and Furhman and Lindsley (1988) for plagioclase (see Berman, 1991 for more details).

File Lake area.—Sample 2026-2 was excluded because $(Na + K + Mn + Ca)_{chlorite}$ 0.07, and sample 2027 because it is garnet-free. Calculation of equilibrium conditions based on water-free assemblages indicates that temperatures determined by the Gt-Chl

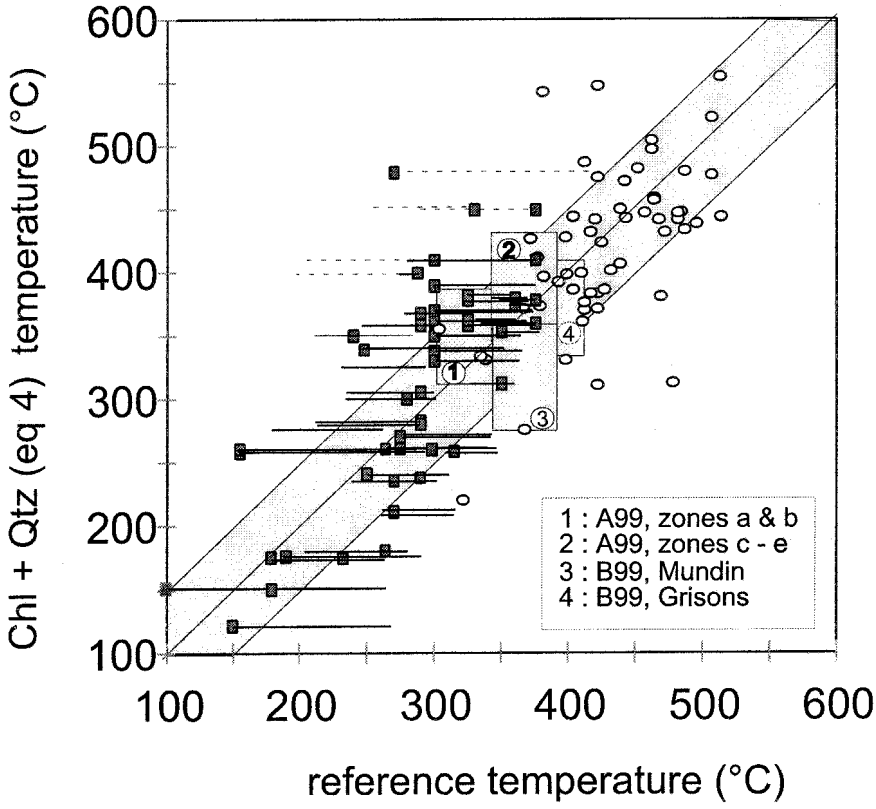

Fig. 12. $T_{(4)}$ versus original T for Car-Chl (large boxes) and low-T Chl-Qtz samples (squares) samples, or temperature calculated with the empirical thermometer from Vidal and others (1999) for Chl-Cld-Qtz samples (circles). The horizontal bars represent the temperature range determined by the original value (square), and those obtained with the empirical thermometers of Cathelineau (1988) and Hillier and Velde (1991).

Fe-Mg exchange reaction are in fair agreement with the previous estimates by Gordon and others (1991) and are consistent with the assumed increase of temperature across the Sill + Bt isograd. However, these temperatures are higher than those determined by the Gt-Bt equilibrium (+35°C for 2025, +40°C for 2038, and +45°C for 1001), and the Chl-Bt exchange reaction is located at unrealistically high pressure (fig. 13A) except for sample 2040-2 (fig. 13B). This sample is the only one for which reasonable P-T conditions with a small scatter are obtained for the H_2O-free Gt-Bt-Chl-Pl-Qtz assemblage (P = 3204 kb (1 σ = 75 bar), T = 573°C (2.1)) calculated from 8 equilibria (3 independent reactions) involving Alm, Pyr, Gros, Daph, Clin, Mg-Am, Phl, Ann, An, and Qtz endmembers (fig. 13A). These results suggest that biotite is equilibrated with chlorite in samples 2040-2 only, or that the chlorite solution properties are not compatible with the biotite solution properties from McMullin (1991). On the contrary, equilibrium between chlorite, garnet, plagioclase, and water ($aH_2O = 1$) was closely achieved in all samples, and the chlorite data calibrated above are compatible with the solution properties from Berman (1990) for garnet and from Furhman and Lindsley (1988) for plagioclase. This is shown by the low scatter (7°-12°C, 0.28-0.52 kb, table 4) of the TWEEQ results based on 14 equilibria (3 independent reactions) for the garnet-chlorite-plagioclase-quartz-H_2O assemblages in samples 1001 and 2025A (fig. 14A) and 29 equilibria (4 independent reactions) for the garnet-chlorite-plagioclase-

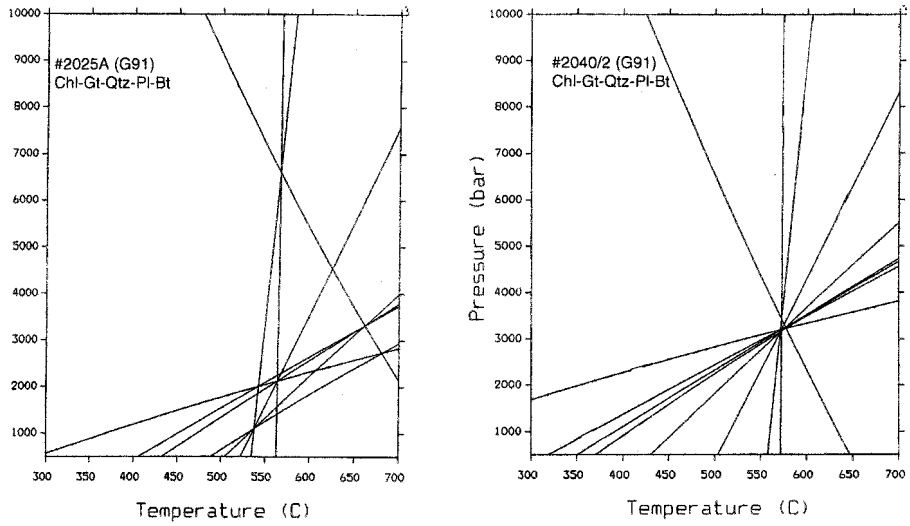

Fig. 13. TWEEQ computation of water-free equilibria among chlorite, garnet, biotite, plagioclase and quartz in the system CaO-MgO-FeO-K_2O-Al_2O_3-SiO_2 calculated for samples 2025A (A) and 2040/2 (B) from File Lake Gordon and others (1991).

quartz-biotite-H_2O assemblage in sample 2040-2 (fig. 14B). Support for the chlorite solution data comes also from the fact that TWEEQ results all plot closely clustered (table 4) and are consistent with previous estimates (Gordon and others, 1991).

Iberian Massif.—Chlorites 6, 9, and 10 were excluded based on chemical criteria. Three assemblages corresponding to different conditions of metamorphism were identified by Arenas and others (1995) : M1 is characterized by the Chl-Gt-Qtz-Ep assemblage, M3 by Chl-Gt-Qtz-Pl, and M4 by Chl-Gt-Qtz-Pl-Bt. Equi-

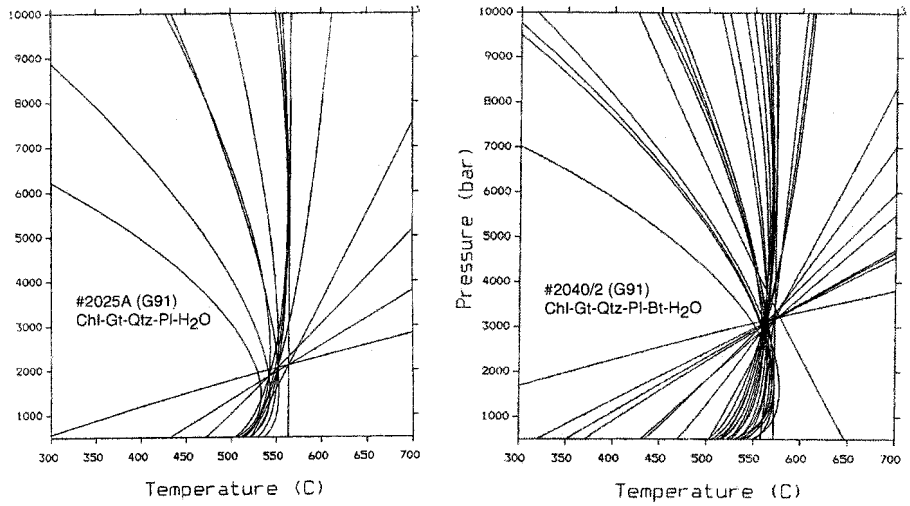

Fig. 14. TWEEQ computation of equilibria among chlorite, garnet, plagioclase, and quartz and H_2O (A) for sample 2025A and chlorite, garnet, plagioclase, biotite, quartz, and H_2O (B) for sample 2040/2 from File Lake (Gordon and others 1991).

librium conditions were estimated for these assemblages (table 4) using the rim composition of garnet.

P-T conditions inferred for mineral assemblages contemporaneous with M1 and M3 from the anhydrous Gt-Chl-Qtz-Ep or Pl assemblages are listed in column "I" (table 4). Except for the pair 3Chl-3Gtr, the temperatures defined by the Gt-Chl equilibrium are in excellent agreement with the previous estimates of Arenas and others (1995), although they are at least 80°C higher than those obtained with various empirical Gt-Chl thermometers, such as that calibrated by Grambling (1990) (column "II" in table 4). The pressure conditions estimated using a simple ideal activity model for epidote ($aCz = XAl^3$) and the standard state properties from Evans (1990) are also in agreement with the previous estimates, except for 3Chl-3Gtr, which are believed to be out of equilibrium. When considering water as an additional phase, the P-T conditions are constrained by 14 equilibria (3 independent reactions). The INTERSX 1σ standard deviation obtained when all equilibria are included is less than 12°C and less than 900 bar for all samples except 3Chl-3Gtr (column "III" in table 4). These results led credence to the equilibrium assumption between garnet, chlorite, epidote or plagioclase and quartz with a fluid of water activity close to unity. They also suggest that the chlorite data are compatible with the clinozoisite data calculated by Evans (1990), garnet data from Berman (1990), and plagioclase from Furhman and Lindsley (1988).

For samples contemporaneous with the M4 metamorphic episode, we report only the results of calculations performed with two biotite compositions (9Bt1 and 2), because the Chl-Bt Fe-Mg exchange reactions calculated with the other biotite compositions are located at unrealistic pressure (above 10 kb), as it was observed for the File Lake samples. For the two assemblages listed in table 4, the calculated P-T conditions are also in good agreement with the previous estimates. In particular, the calculated pressure conditions are clearly lower than in the case of M1 and M3, as was suggested by Arenas and others (1995). Also satisfactory is the relatively low scatter observed when considering chloritoid (XMg = 0.185, XFe = 0.835, Cld7) in addition to the chlorite-garnet-biotite-plagioclase-quartz-H_2O assemblage (169 reactions, 6 independent equilibria).

CONCLUSIONS AND PERSPECTIVES

The Mg-amesite and daphnite standard state properties calculated in the present study are compatible with the thermodynamic data of clinochlore from Berman (1988), Mg-sudoite and -carpholite data from Vidal and others (1992), Fe-chloritoid from Vidal and others (1995), and the Chl-Cld Fe-Mg exchange thermometer of Vidal and others (1999). Selected chlorite-garnet natural data suggest that the chlorite model is also consistent with the solid solution properties from Berman (1990) for garnet, Fuhrman and Lindsley (1988) for plagioclase, and Evans (1990) for epidote. However, large discrepancies are observed between the temperatures obtained from empirical Fe-Mg exchange thermometers and the temperatures calculated in the present study, so that additional work on garnet-chlorite assemblages is required to confirm the apparent consistency between the garnet solid solution model from Berman (1990) and the chlorite model proposed in the present study. The calculated W_{AlMg} and W_{AlFe} parameters are similar in magnitude and sign to the same parameters calculated by Mäder and others (1994) for the M2 site of hornblendes as well as by Aranovitch (1991) for orthopyroxene and by Berman and others (1995) for clinopyroxene. In comparison to other chlorite solution data reported in the literature, our data were calibrated from experimental and natural data covering a wide range of P-T conditions, so that they do not have to be extrapolated outside the calibration range to be used for P-T estimates of natural samples. They are reasonably consistent with the ~60 experimental phase equilibria and solubility experimental constraints obtained by

various authors in the simplified MgO-(FeO)-Al_2O_3-SiO_2-H_2O chemical system as well as most of the 185 natural data used in this study.

At present, the proposed chlorite model only pertains to chlorites with a Si-content < 3. This limit was imposed by the use of clinochlore as the most Si-rich endmember on the serpentine-amesite binary. As a consequence, the model can be used for trioctahedral chlorites that occur in most aluminous metapelites but not for the di/trioctahedral sudoite which often shows a Si-content > 3. An extension of the present model to more siliceous chlorite compositions should be a significant improvement since it would provide additional constraints such as the composition of sudoite and trioctahedral chlorites coexisting at low temperature, medium to low-pressure conditions (see above). In the absence of additional experimental results, these constraints are particularly important to determine more precisely the individual magnitudes of $W\square_{Al}$, $W\square_{Mg}$, and $W\square_{Fe}$ which are poorly constrained at present. However, the extension of the model to more siliceous chlorite compositions will require additional considerations, such as the reciprocal nature of chlorites (Holland and others, 1998) which has been overlooked in the present study.

The use of several chlorite endmembers makes the estimation of paleo-pressure and -temperature conditions possible for high-variance parageneses (> 1) which is not possible when using only one chlorite endmember (classically clinochlore). In particular, reliable pressure estimates can be made for the common Chl-Qtz-Car or Cld or Gt bearing rocks (app.) devoid of aluminosilicates, whereas such estimates are impossible when using only one chlorite endmember. Therefore, it is expected that a more continuous *spatial* assessment of the metamorphic P-T conditions in the field will be possible. Another potential use of the chlorite data calibrated in this study is the calculation of P-T paths using different chlorite generations coexisting in the same thin section. The location of these different generations are often controlled by the rock's microstructure. Therefore, different P-T estimates for various chlorite compositions associated with different structures could be used to constrain the ***P-T-****deformation evolution* from a minimal amount of sample (that is one thin section). Particularly interesting is the use of the chlorite composition to provide constraints on the late stage (in the greenschist facies) shape of the retrograde path followed by HP-LT rocks. Such constraints are generally difficult to obtain since the rock mineralogy does not change significantly at greenschist facies conditions, even though this information is required to build thermomechanical models at the regional scale. Application of examples and a comparison of P-T estimates based on chlorite compositions with estimates based on phengite compositions are discussed in Vidal and Parra (2000).

ACKNOWLEDGMENTS

Thanks are due to P. Agard and R. Bousquet for helpful discussions and for sharing their detailed knowledge of the carpholite-samples used in this study and to R. Oberhänsli for providing chlorite and chloritoid analyses from the Lycian nappes. We are grateful for critical comments by F. Brunet, C. Chopin, and G. Simpson on early drafts of the manuscript and constructive reviews by C. de Capitani, D.M. Jenkins, and an anonymous reviewer.

APPENDIX

Natural data used for the thermodynamic extraction.

The first column lists the molar fraction of atom per site for chlorites (CHL) (see table 1), chloritoid (CLD), and carpholite (CAR).

Column (I) lists the temperature location of equilibrium (4) (not calculated when XSud $<$ 0.045, see text). For the Chl-Cld-Qtz assemblages, $T_{(4)}$ is read at pressure determined by the equilibrium Mg-Sud + Daph + Mg-Am = Fe-Cld + Clin + H_2O when $T_{(4)} < T_{(15)}$ or Mg-Am + Qtz = Mg-Cld + Clin + H_2O when $T_{(4)} > T_{(15)}$ (circles on fig. 9A and B).

Column (II) lists the P-T conditions of the sudoite-absent invariant point where Mg-Am, Clin, Daph, Fe, and Mg-Cld, Qtz, and H_2O coexist (squares on fig. 9A, B and C).

Column (III) lists the temperature estimated with the LnKd (= $(Fe/Mg)^{Cld}/(Fe/Mg)^{Chl}$) = f(T) equation from Vidal and others (1999).

Column IV : Sud-Cld-Qtz-H_2O equilibrium temperature at fixed pressure (4 kb).

(A) Goffé and Bousquet (1997), (B) Bousquet (1998), (C) Cannic and others (1996), (D) Bouybaouène and others (1995), (E) Bröcker and others (1993), (F) Massonne and Schreyer (1989), (G) based on the stability of rectorite + pyrophyllite as determined by Vidal (1997), (H) Oberhänsli and others (2000), (I) Theye and Seidel (1991), Theye and others (1992), (J and L) metapelitic assemblages, (K and M) metabasitic assemblages.

t.s.: this study; A99: Agard (1999); A94: Azanon (1994); AG98: Azanon and Goffé (1997); AE84: Asworth and Ervigen (1984); B98: Bousquet (1998); C85: Cathelineau and Nieva (1985); C79: Chopin (1979); CM84: Chopin and Monie (1984); C93: De caritat and others (1993); G98: Giorgetti and others (1998); G87: Ghent and others (1987); L98: Leoni, Sartori, and Tamponi (1998); OK94: Okay and Kelley (1994); P81: Paradis (1981); T92: Theye and others (1992); R94: Rahn and others (1994); W86: Walshe (1986); HV91: Hillier and Velde (1991); VB98: Vuichard and Ballèvre (1988); V99: Vidal and others (1999).

Appendix tables on following page

Appendix

Natural data used for the thermodynamic extraction

Chlorite-chloritoid-quartz											Sample	I		II		III	Original estimate		Reference
												T	P	T	P	T	T	P	
CHL	[Si	Al]$_{T2}$ [	Mg	Fe	Al	□]$_{M1}$	[Mg	Fe	Al]$_{(M2+M3)}$			°C	Kb	°C	Kb	°C	°C	Kb	
CLD	[Mg	Fe]																	
											Dauphinois zone (Western Alps)								
CHL	.324	.671	.210	.227	.351	.211	.427	.463	.106		Mad-II	355	6	301	6.9	315	300±50	5±2	V99
CLD	.077	.908																	
CHL	.263	.737	.189	.230	.483	.098	.428	.519	.049		Mad-III		P < 0	312	2.8	326			
CLD	.074	.920																	
CHL	.280	.717	.172	.140	.462	.226	.480	.393	.113		Mad-IV		P < 0	255	3.7	273			
CLD	.077	.889																	
CHL	.391	.609	.094	.164	.306	.436	.285	.496	.218		Mad32	275	11	366	10.3	412			ts
CLD	.077	.908																	
											Valaisan zone (Central Alps)								
CHL	.314	.686	.200	.332	.392	.076	.353	.586	.038		CH1	501	11.1	483	11.1	522	500±30(A)	14±1 (A)	B98
CLD	.110	.830																12±2 (B)	
CHL	.334	.665	.302	.255	.340	.102	.511	.433	.051		Chl8	440	11.1	466	12.3	492	470-550	~13 (C)	V99
CLD	.188	.796																	
CHL	.322	.678	.270	.253	.365	.112	.485	.455	.056		Chl6	444	10.1	480	11.6	518			V99
CLD	.180	.780																	
CHL	.323	.676	.284	.250	.365	.101	.502	.441	.051		Chl9	473	8.9	420	9.4	440			V99
CLD	.149	.794																	
CHL	.333	.665	.222	.388	.344	.045	.353	.617	.023		Chl39	552	14.6	511	14.6	541			V99
CLD	.116	.868																	
CHL	.326	.674	.155	.322	.373	.150	.297	.616	.075		chl57	382	7.9	420	9.5	448			V99
CLD	.072	.873																	
CHL	.313	.687	.265	.237	.388	.110	.495	.443	.055		chl56	470	9.4	440	9.7	472			V99
CLD	.165	.795																	
CHL	.321	.679	.229	.335	.369	.067	.392	.573	.034		Fen150	442	12.8	512	12.8	545			ts
CLD	.134	.854																	
CHL	.336	.664	.253	.339	.345	.062	.413	.554	.031		Fen149	437	13.4	494	13.5	515			ts
CLD	.137	.872																	
											Beni Mzala window (Upper sebtides)								
CHL	.336	.662	.343	.196	.346	.115	.598	.341	.058		chl65	440	10.7	418	10.2	438	< 410 (D)	< 8 (D)	V99
CLD	.220	.768																	
CHL	.333	.667	.246	.254	.340	.159	.451	.466	.080		chl34	372	9.4	377	9.6	397			V99
CLD	.117	.880																	
CHL	.328	.672	.269	.248	.352	.132	.483	.445	.066		chl28	425	8	370	6.8	380			V99
CLD	.120	.868																	
CHL	.331	.668	.237	.262	.336	.164	.435	.481	.082		chl39	370	9	420	11	443			V99
CLD	.131	.869																	
CHL	.327	.670	.310	.229	.353	.108	.543	.402	.054		chl64	448	10.8	437	10.5	459	> 430 (D)	> 10 (D)	V99
CLD	.192	.799																	
CHL	.344	.656	.418	.132	.311	.138	.706	.223	.069		chl22X	400	9	430	13.2	452			V99
CLD	.348	.636																	
CHL	.338	.662	.371	.212	.324	.093	.607	.347	.046		chl22	457	12.2	462	12.7	477			V99
CLD	.248	.748																	
											Monte Rosa (Alps)								
CHL	.381	.620	.640	.085	.239	.036	.867	.115	.018		MZ	-	-	504	16.2	501	525±25	16	CM84
CLD	.613	.397																	
											Tinos Island, Greece (Egean domain)								
CHL	.299	.701	.187	.342	.437	.034	.342	.627	.017		k1b/50	-	-	405	6.6	423	440-470 (E)		ts
CLD	.076	.918																	
CHL	.319	.681	.203	.350	.385	.062	.352	.605	.031		k1b/70	520	13.2	505	12.4	542			ts
CLD	.116	.866																	
CHL	.310	.690	.191	.326	.414	.069	.351	.601	.035		k1b/67	545	7.7	420	7.7	443			ts
CLD	.083	.845																	
CHL	.337	.663	.261	.241	.405	.092	.494	.457	.046		IST/172	480	10.3	454	10.3	491			ts
CLD	.169	.785																	
CHL	.322	.678	.268	.258	.386	.088	.485	.468	.044		IST/173	502	10.7	460	10.5	492			ts
CLD	.167	.806																	
											Gran Paradiso (Alps)								
CHL	.380	.620	.475	.186	.257	.082	.689	.270	.041		6-298c	422	14	423	14	440	500±50 (F)	15 (F)	C79,81
CLD	.276	.721																	
CHL	.418	.582	.551	.249	.174	.026	.680	.307	.013		7-172c1	***557***	23	542	21.7	523			C79,81
CLD	.332	.678																	
CHL	.418	.582	.551	.249	.174	.026	.680	.307	.013		7-172c2	***557***	23	488	19.5	467			C79,81
CLD	.291	.719																	
CHL	.418	.582	.613	.152	.170	.065	.776	.192	.033		GP 9	382	15.6	415	17.2	398			C79,81
CLD	.349	.621																	
CHL	.436	.564	.648	.144	.130	.078	.786	.175	.039		GP 12	312	14.2	476	22.1	454			C79,81
CLD	.436	.556																	
CHL	.313	.688	.254	.318	.381	.047	.434	.542	.023		6-80 Chl1	-	-	462	10.2	487			C79,81
CLD	.133	.849																	
CHL	.291	.710	.230	.271	.431	.068	.443	.523	.034		6-80 Chl2	***>600***		426	7.5	456			C79,81
CLD	.127	.856																	
CHL	.314	.686	.270	.293	.396	.042	.467	.508	.021		6-80 Chl3	-	-	416	8.3	434			C79,81
CLD	.127	.856																	
CHL	.380	.618	.490	.199	.236	.076	.684	.278	.038		7-172/2	432	13.5	485	16	487			ts
CLD	.316	.655																	
CHL	.376	.623	.487	.198	.251	.064	.688	.280	.032		7-172/3	478	14.9	485	15.2	488			ts
CLD	.316	.655																	
CHL	.394	.606	.513	.200	.221	.066	.694	.271	.033		7-172/4	440	14.6	480	16.5	476			ts
CLD	.316	.655																	
CHL	.409	.588	.540	.207	.181	.071	.696	.267	.036		7-172/6	380	14	467	17.6				ts
CLD	.290	.641																	
CHL	.408	.591	.536	.218	.193	.054	.692	.281	.027		7-172/11	446	15.5	482	17.3	468			
CLD	.290	.641																	

Appendix

(continued)

Chlorite-chloritoid-quartz										Sample	I		II		III	Original estimate		Reference
											T	P	T	P	T	T	P	
CHL	[Si	Al]$_{T2}$[	Mg	Fe	Al	□]$_{M1}$[Mg	Fe	Al]$_{(M2+M3)}$			°C	Kb	°C	Kb	°C	°C	Kb	
CLD	[Mg	Fe]																
New caledonia																		
CHL	.292	.709	.220	.376	.419	.000	.369	.632	.000	23913.000	-	-	415	7.5	432	410 ± 20	11	G87
CLD	.088	.943																
CHL	.327	.673	.476	.175	.350	.001	.730	.269	.000	37101.000	-	-	480	11.6	496	560 ± 40	12 ± 1	G87
CLD	.370	.676																
Massif Armoricain, France (Hercynian belt)																		
CHL	.294	.706	.124	.288	.419	.169	.274	.638	.084	D44_15	405	6.2	437	7.5	477	330-420 (G)	2	P81
CLD	.069	.844																
CHL	.265	.736	.172	.241	.483	.104	.395	.553	.052	D44_17	540	4	379	4	407			P81
CLD	.088	.855																
Lycian nappes, Turkey (Egean domain)																		
CHL	.423	.578	.370	.131	.160	.339	.612	.217	.170	O.6.3.	220	16	320	15	297	350±30	3±1	AE84
CLD	.187	.801														350±50 (H)	10 (H)	
CHL	.320	.680	.271	.215	.371	.143	.516	.411	.071	O.23.6.	385	8	425	7	396		-	AE84
CLD	.146	.846																
CHL	.322	.678	.278	.186	.356	.179	.544	.364	.089	Chl10	385	9.7	402	10.3	432			ts
CLD	.189	.794								Cld23								
CHL	.325	.674	.301	.188	.348	.162	.565	.353	.081	Chl14	391	10.2	391	10.2	414			ts
CLD	.189	.794								Cld23								
CHL	.361	.637	.318	.200	.284	.198	.552	.347	.099	Chl24	325	10	390	12.6	416			ts
CLD	.185	.799								Cld27								
CHL	.342	.655	.314	.208	.311	.167	.550	.365	.084	Chl25	360	10	409	12	430			ts
CLD	.189	.794								Cld23								
CHL	.338	.662	.300	.208	.324	.168	.541	.375	.084	Chl26	369	9.7	410	11.4	417			ts
CLD	.185	.799								Cld27								
Emilius Klippe (Alps)																		
CHL	.387	.614	.509	.228	.251	.012	.686	.308	.006	ASC16	-	-	537	16	535	550±50	15-20	VB88
CLD	.322	.634																
CHL	.387	.614	.509	.228	.251	.012	.686	.308	.006	ASC16	-	-	526	16.1	523			VB88
CLD	.326	.665																
CHL	.415	.585	.478	.260	.187	.075	.624	.339	.038	AGN6/1	>600		584	25	587			VB88
CLD	.323	.662																
CHL	.375	.625	.522	.212	.269	.003	.712	.289	.002	AGN6	-	-	534	15	535			VB88
Andalusia (Betic chain)																		
CHL	.310	.691	.357	.192	.384	.067	.628	.338	.034	TV903	>600		476	11	503	400-500	8-15	A94, AG97
CLD	.271	.704																
CHL	.323	.677	.184	.345	.383	.088	.333	.623	.044	921c	480	12	450	12	456			A94, AG97
CLD	.085	.905																
CHL	.336	.664	.360	.206	.346	.088	.608	.348	.044	TV21	495	11.5	460	11.5	481			A94, AG97
CLD	.247	.734																
CHL	.332	.668	.275	.179	.354	.192	.548	.356	.096	119	370	10	365	10	388			A94, AG97
CLD	.168	.823																
CHL	.357	.643	.442	.144	.291	.123	.708	.231	.062	Sal56	397	13	397	13	413			A94, AG97
CLD	.301	.663																
CHL	.376	.625	.490	.122	.265	.123	.752	.187	.062	Sal61	375	13	410	15	417			A94, AG97
CLD	.372	.614																
CHL	.347	.654	.413	.192	.335	.061	.662	.308	.030	CONJ-8	>600		415	11	425			A94, AG97
CLD	.249	.743																
CHL	.310	.691	.357	.192	.384	.067	.628	.338	.034	TV903	600	15	472	11	503			A94, AG97
CLD	.271	.704																
CHL	.334	.666	.290	.245	.364	.101	.514	.435	.050	CT2	455	11	462	12	492			A94, AG97
CLD	.188	.796																
Kreta, Hellenides((Egean domain)																		
CHL	.320	.680	.188	.342	.365	.105	.336	.612	.053	k76/54	430	9	415	9	434	350 ± 50	8 ± 2	T92
CLD	.080	.905																
CHL	.385	.615	.465	.145	.230	.160	.701	.219	.080	K86/90	310	12	420	16	428			T92
CLD	.330	.655																
Peloponnese, Hellenides (Egean domain)																		
CHL	.359	.640	.390	.145	.283	.183	.663	.246	.091	Pel34	330	11	337	11	345	450 ± 50(I)	15 ± 2(I)	ts
CLD	.322	.658																
CHL	.347	.651	.460	.120	.304	.115	.737	.193	.058	Pel45	410	15	375	10	380			ts
CLD	.221	.759								43								
CHL	.359	.640	.390	.145	.283	.183	.663	.246	.091	Pel34	333	11.7	333	11.7	345			ts
CLD	.221	.759								43								
CHL	.358	.639	.312	.311	.296	.080	.479	.477	.040	Tg963B24	430	12.5	470	14.3	486			ts
CLD	.163	.837								B2508								
CHL	.326	.674	.278	.278	.351	.094	.475	.475	.047	Tg963B20	445	11.3	455	12.2	504			ts
CLD	.172	.828								B16								
CHL	.302	.698	.220	.263	.411	.105	.429	.513	.053	Tg963B140	475	10.2	505	11.5	563			ts
CLD	.172	.828								B18								
CHL	.346	.651	.297	.288	.307	.109	.478	.463	.054	Tg963B5	398	11.1	408	11.6	420			ts
CLD	.136	.864								B7								
CHL	.336	.662	.269	.299	.342	.090	.451	.501	.045	Tg963B47	445	11.5	480	13	507			ts
CLD	.159	.841								B49								
CHL	.326	.674	.267	.277	.355	.101	.464	.481	.051	Tg963B40	441	11	441	11	465			ts
CLD	.149	.851								B38								
CHL	.361	.636	.340	.274	.283	.103	.522	.420	.051	Tg964M119	395	11.9	380	11.2	378			ts
CLD	.139	.861								M121								
CHL	.345	.653	.331	.271	.307	.091	.521	.426	.046	Tg964M127	442	11.5	402	9.7	407			ts
CLD	.150	.850								M128								
CHL	.346	.654	.330	.273	.318	.079	.523	.433	.040	Tg964N142	485	10.2	410	8.1	414			ts
CLD	.152	.848								N140								
CHL	.362	.636	.341	.279	.290	.089	.524	.429	.044	Tg964N137	426	11.4	396	10.4	398			ts
CLD	.145	.855								N136								
CHL	.267	.730	.255	.291	.475	.001	.469	.537	.001	7ch1/III	-	-	515	9.2	572	505-540	6.5-9	A95
CLD	.185	.830								7cl1								
CHL	.320	.677	.291	.322	.357	.031	.467	.516	.015	8ch1/III	-	-	458	10.4	474			A95
CLD	.140	.825								8cl1								

Appendix
(continued)

Chlorite-carpholite-quartz											Sample	I		Original estimate		Reference
	[Si	Al]$_{T1}$	[Mg	Fe	Al	□]$_{M1}$	[Mg	Fe	Al]$_{(M2+M3)}$			T °C	P kb	T °C	P kb	
CHL	.366	.630	.252	.390	.269	.089	.374	.579	.045		Rf941/F15	337	15	300-350	10-15	A99
CAR	.440	.560														
CHL	.365	.635	.264	.322	.287	.127	.420	.512	.064		Rf942/F54	332	12.5			A99
CAR	.440	.560														
CHL	.366	.630	.252	.390	.269	.089	.374	.579	.045		Rf943/F38	338	15			A99
CAR	.440	.560														
CHL	.333	.666	.192	.400	.334	.074	.307	.639	.037		Pit944/J14	395	16.4			A99
CAR	.320	.580														
CHL	.361	.639	.232	.252	.297	.219	.422	.459	.109		Gb944/O31	304	10.3			A99
CAR	.450	.550														
CHL	.344	.655	.205	.355	.316	.125	.342	.594	.062		J874/H50	337	13.7			A99
CAR	.420	.580														
CHL	.365	.632	.236	.412	.271	.081	.345	.602	.040		Ccs951/J35	347	15.5			A99
CAR	.380	.620														
CHL	.374	.621	.206	.459	.263	.073	.297	.663	.036		Vaz951/L31	340	16			A99
CAR	.322	.688														
CHL	.353	.645	.252	.313	.313	.123	.417	.519	.061		Vaz951/L33	351	12.9			A99
CAR	.435	.565														
CHL	.369	.629	.249	.406	.283	.063	.366	.596	.031		Des952/M26	391	16.5			A99
CAR	.332	.678														
CHL	.339	.661	.292	.277	.326	.105	.486	.462	.053		Bo955/N57	385	14.2			A99
CAR	.542	.458														
CHL	.348	.650	.295	.323	.305	.077	.457	.500	.039		Bo951/J24	394	16.2			A99
CAR	.530	.470														
CHL	.352	.648	.305	.306	.300	.089	.476	.477	.045		Mor954/J18	382	14.9	350-400	12-17	A99
CAR	.520	.480														
CHL	.353	.647	.239	.402	.305	.053	.354	.595	.027		Mor951/J66	415	18.5			A99
CAR	.371	.629														
CHL	.394	.605	.532	.181	.213	.074	.718	.244	.037		Pel943/K4	403	14.9			A99
CAR	.722	.288														
CHL	.354	.645	.221	.395	.296	.088	.337	.602	.044		Pit943/M1	362	14.5			A99
CAR	.322	.688														
CHL	.365	.633	.310	.347	.279	.064	.450	.505	.032		Ge951/M48	403	16.6			A99
CAR	.442	.55														
CHL	.375	.622	.285	.361	.280	.074	.421	.532	.037		Ge951/M51	365	16.3			A99
CAR	.500	.500														
Mundin unit, Engadine window (Central Alps)																
CHL	.402	.595	.181	.127	.609	.083	.534	.373	.083		Alp938a/7	432	11.8	350-400	11-13 (J) 10-12 (K)	B99
CAR	.500	.500														
CHL	.404	.596	.385	.191	.205	.218	.595	.295	.109		Alp944/7	262	10.1			B99
CAR	.720	.280														
CHL	.398	.602	.406	.227	.216	.150	.589	.330	.075		Samp935/4	298	11.2			B99
CAR	.640	.360														
CHL	.355	.644	.350	.218	.342	.090	.547	.340	.045		Saro942a/12	420	15.3			B99
CAR	.620	.380														
CHL	.395	.603	.385	.208	.222	.185	.588	.317	.093		Nau947/2	285	10.5			B99
CAR	.647	.320														
CHL	.356	.644	.372	.206	.306	.115	.604	.335	.058		Nau947/3	382	13.5			B99
CAR	.690	.268														
CHL	.422	.577	.383	.187	.212	.218	.597	.292	.109		Nau947/4	263	9.6			B99
CAR	.645	.311														
CHL	.376	.622	.439	.208	.263	.090	.647	.307	.045		Nau947/5	394	14.2			B99
CAR	.670	.290														
CHL	.389	.611	.386	.198	.246	.170	.602	.308	.085		Nau947/6	308	10.8			B99
CAR	.649	.312														
CHL	.357	.643	.365	.212	.292	.131	.590	.343	.066		Nau947/7	363	12.4			B99
CAR	.623	.337														
CHL	.379	.621	.398	.217	.252	.133	.601	.329	.066		Eng9315b/13	339	11.8			B99
CAR	.607	.291														
CHL	.367	.631	.389	.243	.276	.091	.585	.366	.046		Eng9315b/15	382	14.7			B99
CAR	.670	.120														
CHL	.413	.587	.370	.211	.228	.191	.574	.327	.096		Eng9315b/16	280	10.1			B99
CAR	.610	.390														
CHL	.371	.627	.418	.202	.265	.115	.632	.306	.057		Eng9315b/18	368	12.8			B99
CAR	.650	.350														
CHL	.355	.644	.345	.264	.300	.090	.537	.411	.045		Cha931/2	392	15.1			B99
CAR	.621	.379														
CHL	.411	.589	.408	.222	.212	.159	.594	.323	.079		Eng942/3	289	10.7			B99
CAR	.621	.000														
CHL	.406	.593	.430	.181	.196	.193	.635	.268	.097		Eng942/4	272	9.9			B99
CAR	.690	.268														
CHL	.362	.638	.391	.244	.285	.081	.588	.367	.040		Tun941/1	421	17.7			B99
CAR	.527	.403														
CHL	.357	.643	.365	.260	.299	.075	.558	.398	.038		Eng942/2	326	11.5			B99
CAR	.499	.466														
CHL	.373	.627	.388	.248	.275	.089	.581	.371	.044		Eng942/3	391	14.3			B99
CAR	.580	.380														
CHL	.369	.630	.385	.267	.269	.078	.564	.391	.039		Eng942/13	407	14.6			B99
CAR	.499	.466														

Appendix

(continued)

Chlorite-carpholite-quartz											Sample	I		Original estimate		Reference
												T	P	T	P	
CHL	[Si	Al]$_{T2}$[	Mg	Fe	Al	□]$_{M1}$[Mg	Fe	Al]$_{(M2+M3)}$				°C	kb	°C	kb	
CAR	[Mg	Fe]														
Grison (upper unit), Engadine window (Central Alps)																
CHL	.354	.646	.271	.332	.312	.085	.428	.524	.043		Prasug941/4	376	15.8	350-400 (1)	12-16 (L)	B99
CAR	.526	.484													11-13 (M)	
CHL	.365	.632	.275	.338	.270	.117	.420	.517	.059		Prasug941/5	324	13.5			B99
CAR	.502	.498														
CHL	.351	.648	.264	.321	.306	.109	.425	.516	.054		Prasug941c/3	353	14.4			B99
CAR	.530	.470														
CHL	.351	.648	.264	.321	.306	.109	.425	.516	.054		Prasug941c/33	355	14.2			B99
CAR	.505	.467														
											Saf942b/1	379	14.6			B99
CHL	.346	.653	.281	.313	.311	.095	.447	.498	.048		Chur941d/4	379	14.5			B99
CAR	.483	.477														
CHL	.332	.667	.254	.310	.339	.098	.426	.520	.049		Chur941d/5	390	14.8			B99
CAR	.480	.520														
CHL	.358	.641	.237	.288	.344	.131	.421	.512	.066		Chur941b/3	351	13.2			B99
CAR	.510	.490														
CHL	.345	.654	.253	.312	.311	.124	.417	.515	.062		Tomil940/6	347	13.4			B99
CAR	.491	.509														
CHL	.327	.673	.273	.238	.358	.130	.500	.435	.065		Vers941a/2	397	12.3			B99
CAR	.460	.540														
CHL	.369	.630	.385	.267	.269	.078	.564	.391	.039		Vers941a/13	398	15.3			B99
CAR	.580	.420														

Chlorite-quartz (low-T samples)											I	C88	HV91	Original estimate	
											T	T	T	T	
CHL	[Si	Al]$_{T2}$[	Mg	Fe	Al	□]$_{M1}$[Mg	Fe	Al]$_{(M2+M3)}$			°C	°C	°C	°C	
CHL	.453	.548	.156	.440	.095	.309	.220	.623	.154		1	175	291	190	190	W86
CHL	.457	.542	.404	.382	.084	.130	.477	.451	.065		8	260	287	264	264	W86
CHL	.468	.532	.351	.332	.064	.253	.448	.424	.126		6	180	281	264	264	W86
CHL	.440	.561	.326	.452	.121	.101	.393	.545	.050		7	300	299	280	280	W86
CHL	.448	.553	.359	.401	.105	.135	.436	.487	.067		11	258	294	315	315	W86
CHL	.321	.679	.208	.295	.358	.139	.384	.546	.070		CV	410	375	375	375	L98
CHL	.325	.674	.221	.266	.349	.163	.417	.501	.082		MF	378	375	375	375	L98
CHL	.324	.675	.209	.272	.351	.167	.398	.518	.084		MG	370	373	325	325	L98
CHL	.339	.661	.208	.253	.322	.217	.402	.490	.109		CT	338	364	300	300	L98
CHL	.376	.623	.200	.250	.246	.304	.377	.471	.152		BVG	260	340	275	275	L98
CHL	.314	.686	.217	.295	.372	.116	.399	.543	.058		cv12	450	380	375	375	L98
CHL	.338	.662	.205	.296	.324	.176	.373	.539	.088		cv89	360	364	375	375	L98
CHL	.328	.672	.215	.283	.345	.158	.397	.524	.079		cv83	378	371	375	375	L98
CHL	.327	.673	.198	.259	.347	.196	.390	.512	.098		mf1	358	372	325	325	L98
CHL	.351	.649	.321	.236	.299	.145	.534	.393	.072		mf19	382	356	325	325	L98
CHL	.344	.657	.250	.262	.313	.174	.446	.466	.087		mf63	363	361	325	325	L98
CHL	.322	.677	.217	.273	.354	.155	.408	.514	.078		mg67	390	374	300	300	L98
CHL	.327	.673	.200	.287	.345	.168	.376	.540	.084		mg45	370	371	300	300	L98
CHL	.332	.668	.215	.255	.335	.194	.413	.490	.097		mg33	361	368	300	300	L98
CHL	.339	.661	.227	.255	.322	.197	.424	.477	.098		ct7	350	364	300	300	L98
CHL	.339	.662	.189	.250	.324	.238	.379	.502	.119		ct19	330	364	300	300	L98
CHL	.372	.628	.177	.233	.257	.332	.360	.474	.166		bvg12	270	343	275	275	L98
CHL	.381	.619	.223	.264	.238	.275	.394	.468	.138		bvg32	270	337	275	275	L98
CHL	.345	.655	.247	.178	.309	.265	.499	.360	.133		M34	312	360	350	350	G98
CHL	.318	.682	.198	.238	.364	.200	.408	.491	.100		M655	374	377	360	360	G98
CHL	.331	.668	.237	.262	.336	.164	.435	.481	.082		chl39	380	368	360	360	G98
CHL	.365	.635	.077	.393	.270	.260	.143	.727	.130		ON-5	257	347	155	155	C93
CHL	.427	.573	.339	.405	.169	.087	.430	.512	.044		Mf776	358	307	290	290	R94
CHL	.483	.517	.366	.448	.068	.118	.418	.511	.059		MF778	240	271	290	290	R94
CHL	.461	.539	.391	.390	.107	.112	.467	.467	.056		MRT96	282	285	290	290	R94
CHL	.396	.604	.323	.333	.232	.113	.461	.475	.056		MRT17	368	327	290	290	R94
CHL	.434	.561	.353	.373	.156	.117	.452	.478	.059		MRT24	305	300	290	290	R94
CHL	.490	.510	.498	.279	.041	.182	.579	.324	.091		ca1	175	266	180	180	CN85
CHL	.499	.501	.461	.248	.041	.249	.566	.305	.125		ca2	150	261	180	180	CN85
CHL	.463	.537	.579	.234	.100	.086	.674	.272	.043		ca5	350	284	240	240	CN85
CHL	.473	.527	.616	.263	.070	.052	.680	.290	.026		ca9	400	277	290	290	CN85
CHL	.496	.504	.606	.294	.031	.069	.645	.313	.035		ca10	275	263	290	290	CN85
CHL	.469	.531	.541	.325	.086	.049	.605	.363	.024		ca13	410	280	300	300	CN85
CHL	.485	.512	.538	.323	.048	.091	.594	.356	.045		ca14	260	268	300	300	CN85
CHL	.320	.684	.169	.299	.381	.151	.334	.589	.075		44	353	378	350	350	CN85
CHL	.495	.508	.241	.390	.063	.305	.324	.523	.153		7036-64	150	265	100	100	HV91
CHL	.338	.644	.203	.346	.292	.160	.340	.580	.080		7036-58	340	353	250	250	HV91
CHL	.386	.616	.265	.404	.261	.070	.379	.577	.035		824-3b	450	334	330	330	HV91
CHL	.490	.510	.229	.356	.045	.370	.314	.488	.185		ch228	120	266	150	150	HV91
CHL	.422	.577	.260	.292	.180	.267	.405	.454	.134		ch139	240	310	250	250	HV91
CHL	.413	.595	.052	.285	.229	.434	.119	.654	.217		b12	210	321	270	270	HV91
CHL	.411	.590	.038	.398	.206	.358	.072	.748	.179		a3	210	318	270	270	HV91
CHL	.435	.565	.318	.326	.136	.220	.437	.447	.110		119	235	302	270	270	HV91
CHL	.260	.740	.056	.338	.491	.115	.134	.808	.058		d16	480	415	270	270	HV91

Sudoite-chloritoid-quartz												IV		
												T	P (fixed)	
SUD	[Si	Al]$_{T2}$[	Mg	Fe	Al	□]$_{M1}$[Mg	Fe	Al]$_{(M2+M3)}$				°C	kb	
CLD	[Mg	Fe]												
Lycian nappes														
SUD	.501	.498	.105	.028	.002	.869	.445	.120	.434		Lyc11	343	4	t.s.
CLD	.189	.794												
SUD	.505	.495	.069	.015	.000	.922	.440	.095	.461		Lyc13	316	4	t.s.
CLD	.189	.794												
Peloponese														
SUD	.505	.495	.069	.015	.000	.922	.440	.095	.461		Tg972-4/64	375	4	t.s.
CLD	.281	.719									65			
SUD	.492	.505	.066	.014	.012	.908	.447	.097	.454		Tg972-4/67	397	4	t.s.
CLD	.345	.655									48			

References

Agard, P., ms, 1999, Evolution métamorphique et structurale des métapélites océaniques dans l'orogénèse Alpin : l'exemple des Schistes Lustrés des Alpes occidentales (Alpes Cottiennes) : Ph.D., Université Paris 6, 295 p.

Ahn, J. H. and Peacor, D. R., 1985, Transmission electron microscopic study of diagenetic chlorite in Gulf Coast argillaceous sediments : Clays and Clay Mineral, v. 33, p.—236.

Aranovitch, L. Ya, 1991, Mineral equilibria of multicomponent solid solutions, Nauka Press, Moscow, 253p. (in Russian)

Arenas, R., Rubio Pascual, F. J., Diaz Garcia, F. and Martinez Catalan, J. R., 1995, High-pressure micro-inclusions and development of an inverted metamorphic gradient in the Santiago Schists (Ordenes Complex, NW Iberian Massif, Spain) : evidence of subduction and syncollisional decompression : Journal of Metamorphic Geology, v. 13, p.141–164.

Ashworth, J. R., and Evirgen, M. M., 1984, Mineral chemistry of regional chloritoid assemblages in the Chlorite Zone, Lycian Nappes, South-west Turkey : Mineralogical Magazine, v. 48, p.159–165.

Azañón, J. M., 1994, Metamorphismo de alta presión/baja temperatura, baja presión/alta temperatura y tectónica del complejo Alpujàrride (Cordilleras Bético-Rifeñas). Tesis Doctoral, Granada, Spain.

Azañón, J. M., and Goffé, B., 1997, High-pressure, low-temperature metamorphic evolution of the central Alpujarrides, Betic Cordillera (SE Spain) : European Journal of Mineralogy, v. 9, p. 1035–1051.

Bailey, S. W., 1988, Chlorites : structures and crystal chemistry, in Bailey, S.W., editor, Hydrous Phyllosilicates : Review in Mineralogy, v. 19, p. 347–403.

Baker, J. and Holland, T. J. B., 1996, Experimental reversals of chlorite compositions in divariant MgO-Al_2O_3-SiO_2-H_2O assemblages : implications for order-disorder in chlorites : American Mineralogist, v. 81, p. 676–684.

Berman, R. G., 1988, Internally-Consistent Thermodynamic Data for Minerals in the system Na_2O-K_2O-CaO-MgO-FeO-Fe_2O_3-Al_2O_3-SiO_2-TiO_2-H_2O-CO_2 : Journal of Petrology, v. 29, p. 445–522.

——— 1990, Mixing properties of Ca-Mg-Fe-Mn garnets : American Mineralogist, v. 75, p. 328–344.

——— 1991, Thermobarometry using multi-equilibrium calculations : a new technique, with petrological applications : Canadian Mineralogist, v. 29, p. 833–855.

Berman, R. G., Aranovitch, L. Y., and Pattison, D. R. M., 1995, Reanalysis of the garnet - clinopyroxene Fe-Mg exchange thermometer. II. Thermodynamic analysis. Contributions to Mineralogy and Petrology, v. 119, p. 30–42.

Berman, R. G. and Brown, T. H., 1984, A thermodynamic model for multicomponent melts, with application to the system CaO-Al_2O_3-SiO_2 : Geochimica et Cosmochimica Acta, v. 48, p. 661–678.

——— 1985, The heat capacity of minerals in the system K_2O-Na_2O-CaO-MgO-FeO-Fe_2O_3-Al_2O_3-SiO_2-TiO_2-H_2O-CO_2: representation, estimation, and high temperature extrapolation : Contributions to Mineralogy and Petrology, v. 89, p. 168–183.

Berman, R. G., Engi, M., Greenwood, H. J., and Brown, T. H., 1986, Derivation of internally-consistent thermodynamic data by the technique of mathematical programming, a review with application to the system MgO-SiO_2-H_2O : Journal of Petrology, v. 27, p. 1331–1364.

Black, P. M., 1975, Mineralogy of New Caledonia metamorphic rocks : IV. Sheet silicates from the Ouégoa District : Contributions to Mineralogy and Petrology , v. 49, p. 269–284.

Bousquet, R., ms, 1998, L'exhumation des roches métamorphiques de haute pression-basse température : de l'étude de terrain à la modélisation numérique. Exemple de la fenêtre de l'Engadine et du domaine Valaisan dans les Alpes Centrales : Ph.D., Université Paris XI., 279 p.

Bouybaouène, M. L., Goffé, B., and Michard, A., 1995, High-pressure, low-temperature metamorphism in the Sebtides nappes, northern Rif, Morocco, Geogaceta, v. 17, 117–119.

Bröcker, M., Kreutzer, H., Matthews, H., and Okrush, M., 1993, $^{40}Ar/^{39}Ar$ and Oxygen isotop studies of polymetamorphism from Tinos Island, Cycladic blueschist belt, Greece : Journal of Metamorphic Geology, v. 11, p. 223–240.

Bryndzia, L. T., and Scott, L. D., 1987, The composition of chlorite as a function of sulfur and oxygen fugacity; an experimental study : American Journal of Science, v. 287, p. 50–76.

Cannic, S., Lardeaux, J. M., Mugnier, J. L., and Hemandez, J., 1996, Tectono-metamorphic evolution of the Roignais-Versoyen Unit (Valaisan domain, France) : Eclogae geologicae Helvetiae, v. 89, 321–343.

Cathelineau, M., 1988, Cation site occupancy in chlorites and illites as a function of temperature : Clay Minerals, v. 23, 471–485.

Cathelineau, M., and Nieva, D., 1985, A chlorite solid solution geothermometer. The Los Azufres (Mexico) geothermal system : Contributions to Mineralogy and Petrology , v. 91, p. 235–244.

Chopin, C., ms, 1979, De la Vanoise au massif du Grand Paradis, une approche pétrographique et radiochronologique de la signification géodynamique du métamorphisme de haute pression. Ph.D., Université Paris VI, 145 pp.

——— 1981, Talc-Phengite: a widespread assemblage in high-grade pelitic blueschists of the western Alps : Journal of Petrology, v. 22, p. 628–650.

Chopin, C., and Monié, P., 1984, A unique magnesiochloritoid-bearing; high-pressure assemblage from the Monte Rosa, western Alps: petrologic and ^{40}Ar-^{39}Ar radiometric study : Contributions to Mineralogy and Petrology, v. 87, p. 388–398.

Chopin, C., and Schreyer, W., 1983, Magnesiocarpholite and magnesiochloritoid: Two index minerals of pelitic blueschists and their preliminary phase relations in the model system MgO-Al_2O_3-SiO_2-H_2O : American Journal of Science, 283-A, p. 72–96.

Comodi, P., Mellini, M., and Zanazzi, P.F., 1992, Magnesiochloritoid: compressibility and high pressure structure refinement : Physics and Chemistry of Minerals, v. 18, p. 483–490.

Cooper, A. F., 1972, Progressive metamorphism of metabasic rocks from the Haast Schist Group of southern New Zealand :Journal of Petrology , v.13, p. 457–492.
Curtis, C. D., Hughes, C. R., Whiteman, J. A., and Whittle, C. K., 1985, Compositional variation within some sedimentary chlorites and some comments on their origin : Mineralogical Magazine, v.49, p. 375–386.
Davis, P. K. and Navrotsky, A., 1983, Quantitative correlations of deviations from ideality in binary and pseudo-binary solid solutions: Journal of solid state chemistry, v. 46, p. 1–22.
Decaritat, P., Hutcheon, I., and Walshe, J. L., 1993, Chlorite geothermometry : a review : Clays and clay minerals, v. 41, p. 219–239.
Dyar, M. D., Guidotti, C. V., Harper, G. D., McKibben, M. A., and Saccocia, P. J., 1992, Controls on ferric iron in chlorite : Geological Society of America, Abstracts with Programs, v. 24, p. 130.
Ernst, W. G., Seki, I., Onuki, H., and Gilbert, M. C., 1970, Comparative study of low-grade metamorphism in the California coast range and the outer metamorphic belt of Japan : Geological Society of America, v. 124, p. 1–259.
Evans, B. W., 1990, Phase relations in epidote-blueschists : Lithos, v. 25, p. 3–23.
Franceschelli, M., Mellini, M., and Ricci, C. A., 1989, Sudoite, a rock-forming mineral in Verrucano of the Northern Appenines (Italy) and the sudoite-chloritoid-pyrophyllite assemblage in prograde metamorphism : Contributions to Mineralogy and Petrology , v. 101, p. 274–279.
Fransolet, A. M., and Schreyer, W., 1984, Sudoite, di/trioctahedral chlorite : a stable low-temperature phase in the system MgO-Al2O3-SiO2-H2O : Contributions to Mineralogy and Petrology, v. 86, p. 409–417.
Furhman, M. L., and Lindsey, D. H., 1988, Ternary-felspar modeling and thermometry : American Mineralogist, v. 73, p. 201–215.
Ghent, E. D., Stout, M. Z., Black, P. M., and Brothers, R. N., 1987, Chloritoid bearing rocks associated with blueschists and eclogites, northern New Caledonia : Journal of Metamorphic Geology, v. 5, p. 239–254.
Giorgetti, G., Goffé, B., Memmi, I., and Nieto, F., 1998, Metamorphic evolution of Verrucano metasediments in northern Apennines : new petrological constraints : European Journal of Mineralogy, v.10, p. 1295–1308.
Goffé, B., and Bousquet, R., 1997, Ferrocarpholite, chloritoïde et lawsonite dans les métapélites des unités du Versoyen et du Petit St Bernard (zone valaisanne, Alpes occidentales) : Schweizerische Mineralogische und Petrogrographische Mitteilungen, v. 77, p. 137–147.
Gordon, T. M., Ghent, E. D., and Stout, M. Z., 1991, Algebraic analysis of the biotite-sillimanite isograd in the File Lake area, Manitoba : Canadian Mineralogist, v. 29, p. 673–686.
Grambling, J. A., 1990, Internally-consistent geothermometry and H_2O barometry in metamorphic rocks; the example garnet-chlorite-quartz : Contributions to Mineralogy and Petrology, v. 105, p. 617–628.
Hillier, S., and Velde, B., 1991, Octahedral occupancy and the chemical composition of diagenetic (low-temperature) chlorites : Clay Minerals, v. 26, p. 146–168.
Holland, T. J. B., 1989, Dependance of entropy on volume for silicates and oxide minerals, a review and a predictive model : American Mineralogist, v. 74, p. 5- 13.
Holland, T. J. B., Baker, J., and Powell, R., 1998, Mixing properties and activity-composition relationships of chlorites in the system MgO-FeO-$A1_2O_3$-SiO_2-H_2O : European Journal of Mineralogy, v. 10, 395–406.
Jenkins, D. M., and Chernosky, J. V., 1986, Phase equilibria and crystallochemical properties of Mg-chlorites : American Mineralogist, v. 71, p. 924–936.
Jiang, W. J., Peacor, D. R., and Buseck, P. R., 1994, Chlorite geothermometry ?-contamination and apparent octahedral vacancies : Clays and Clay Minerals, v. 42, p. 593–605.
Jowett, E. C., 1991, Fitting iron and magnesium into the hydrothermal chlorite geothermometer : GAC/MAC/SEG Joint Annual Meeting (Toronto), Program with Abstracts, 16, A62.
Kranidiotis, P., and Mac Lean, W. H., 1987, Systematics of chlorite alteration at the Phelps Dodge massive sulfide deposit, Matagami, Quebec : Economic Geology, v. 82, p. 1898–1911.
Laird, J., 1988, Chlorites: metamorphic petrology, in Bailey, S.W., editor, Hydrous Phyllosilicates : Review in Mineralogy, v. 19, 406–453.
Leoni, L., Sartori, F., and Tamponi, M., 1998, Compositional variation in K-white micas and chlorites coexisting in Al- saturated metapelites under late diagenetic to low-grade metamorphic conditions (Internal Liguride Units, Nortern Apennines, Italy) : European Journal of Mineralogy, v. 10, p. 1321–1339.
Mäder, U. K., Percival, J. A., and Berman, R. G., 1994, Thermobarometry of garnet-clinopyroxene-hornblende granulites from the Kapuskasing structural zone : Canadian Journal of Earth Sciences, v. 31, p. 1134–1145.
Massonne, H. J., 1989, The upper thermal stability of chlorite + quartz : an experimental study in the system MgO-Al_2O_3-SiO_2-H_2O : Journal of Metamorphic Geology, v. 7, p. 567–581.
McDowell, S. D., and Elders, W. A., 1980, Authigenic layer silicate minerals in borehole Emore 1, Salton Sea Geothermal Field, California, USA : Contributions to Mineralogy and Petrology , v. 74, p. 293–310.
McMullin, D. W. A., Berman, R. G., and Greenwood, H. J., 1991, Calibration of the SGAM thermobarometer for pelitic rocks using data from phase-equilibrium experiments and natural assemblages : Canadian Mineralogist, v. 29, p. 889–908.
McPhail, D., Berman, R. G., and Greenwood, H. J., 1990, Experimental and theoretical constraints on aluminium substitutions in magnesian chlorite, and a thermodynamic model for H_2O in magnesian cordierite : Canadian Mineralogist, v. 28, p. 859–874.
Moine, B., Gavoille, B., and Thiebaut, J., 1982, Géochimie des transformations métasomatique à l'origine du gissement à talc et chlorite de Trimouns (Luzenac, Ariège, France) : Bulletin de Minéralogie, v. 105, p. 62–75.
Montoya, J. W. and Hemley, J. J., 1975, Activity relations and stabilities in alkali feldspar and mica alteration reactions : Economic Geology and the Bulletin of the Society of Economic Geologists, v.70, 577–583.

Nelson, D. O., and Guggenheim, S., 1993 , Inferred limitations to the oxidation of Fe in chlorite : a high-temperature single-crystal X-ray study : American Mineralogist, v. 78, p. 1197–1207.
Oberhänsli, R., Partzsch, J., Canadan, O., and Cetinkaplan, M., 2000, First occurrence of Fe-Mg-carpholite documenting a High Pressure metamorphism in metasediments of the Lycian Nappes, SW Turkey : Geologische Rundschau., In press.
Okay, A. I., and Kelley, S. P., 1994, Tectonic setting, petrology and geochronology of jadeite + glaucophane and chloritoid + glaucophane schists from north-west Turkey : Journal of Metamorphic Geology, v. 12, p. 455–466.
Paradis, S., ms, 1981, Le métamorphisme Hercynien dans le domaine centre Armoricain Occidental. Ph.D., Université Bretagne occidentale, 224 p.
Rahn, M., Mullis, J., Erdelbrock, K., and Frey, M., 1994, Very low-grade metamorphism of the Taveyanne greywacke, Glarus Alps, Switzerland : Journal of Metamorphic Geology, v. 12, p. 625–641.
Saccocia, P. J., and Seyfried, W., 1994, The solubility of chlorite solid solutions in 3.2wt% NaCl fluids from 300–400°C, 500 bars : Geochimica and Cosmochimica Acta, v. 58, p. 567–585.
Schreyer, W., Mendenbach, O., Abraham, K., Gebert, W., and Müller, W. F., 1982, Kulkeite, a new metamorphic phyllosilicate mineral : ordered 1:1 chlorite/talc mixed-layer : Contributions to Mineralogy and Petrology , v. 80, p. 103–109.
Shirozu, H., 1978, Chlorite minerals, in Sudo, T., and Shimoda, S., editors, Clays and Clay Minerals of Japan : Amsterdam, The Netherlands, Elsevier, p. 243–264.
Spear, F. S. and Cheney, J. T., 1989, A petrogenetic grid for pelitic schists in the system SiO_2–Al_2O_3-FeO-MgO-K_2O-H_2O : Contributions to Mineralogy and Petrology, v. 101, 149–164.
Staudigel, H., and Schreyer, W., 1977, The upper thermal stability of clinochlore, $Mg_5Al[Si_3Al_{10}](OH)_8$, at 10–35 kbar $P(H_2O)$: Contributions to Mineralogy and Petrology, v. 61, 187–198.
Sverjensky, D. A., Hemley, J. J., and D'Angelo, W. M., 1991, Thermodynamic assessment of hydrothermal alkali feldspar-mica-aluminosilicate equilibria : Geochimica et Cosmochimica Acta, v. 55, 989–1004.
Theye, T., and Seidel, E., 1991, Petrology of low-grade high-pressure metapelites from the Extemal Hellenides (Crete, Peloponnese). A case study with attention to sodic minerals : European Journal of Mineralogy, v. 3, p. 343–366.
Theye, T., Seidel, E., and Vidal, O., 1992, Carpholite, sudoite, and chloritoid in low-grade high pressure metapelites from Crete and the Peloponnese, Greece : European Journal of Mineralogy, v. 4, p. 487–507.
Vidal, O., 1997, Experimental study of the thermal stability of pyrophyllite, paragonite, and sodic clays in a thermal gradient : European Journal of Mineralogy, v. 9, p. 123–140.
Vidal, O., Goffé, B., Parra, T., Bousquet, R., 1999, Calibration and testing of an empirical chloritoid-chloriteMg-Fe thermometer and thermodynamic data for daphnite : Journal of Metamorphic Geology, v. 17, p. 25–39.
Vidal, O., Goffé, B., and Theye, T., 1992, Experimental study of the stability of sudoite and magnesiocarpholite and calculation of a new petrogenetic grid for the system FeO-MgO-$A1_2O_3$-SiO_2-H_2O : Journal of metamorphic Geology, v. 10, p. 603–614.
Vidal, O., and Parra, T., 2000, Exhumation paths of high pressure metapelites obtained from local equilibria for chlorite-phengite assemblages : Geological Journal, v. 35(3/4), p. 139–161.
Vidal, O., Theye, T., and Chopin, C., 1994, Experimental study of chloritoid stability at high pressure and various fO_2 conditions : Contributions to Mineralogy and Petrology, v. 118, p. 256–270.
Vieillard, P., 1994, Prediction of enthalpy of formation baszed on refined crystal structures of multisite compounds : Part2. Application to minerals belonging to the system Li_2O-Na_2O-K_2O-BeO-MgO-CaO-MnO-FeO-Fe_2O_3-Al_2O_3-SiO_2-H_2O. Results and discussion : Geochimica et Cosmochimica Acta, v. 58, p. 4065–4107.
Vuichard, J. P., and Ballèvre, M., 1988, Garnet chloritoid equilibria in eclogitic pelitic rocks from the Sezia zone (Western Alps): their bearing on phase relations in high pressure metapelites : Journal of metamorphic Geology, v. 6, p. 135–157.
Walshe, J. L., 1986, A six-component chlorite solid solution model and the conditions of chlorite formation in hydrothermal and geothermal systems : Economic Geology, v. 81, p. 681–703.
Walshe, J. L., and Solomon, M., 1981, An investigation into the environement of formation of volcanic-hosted Mt. Lyell copper deposits, using geology, mineralogy, stable isotopes, and a six-component chlorite solid-solution model : Economic Geology, v. 76, p. 246–284.
Zane, A., and Sassi, R., 1998, New data on metamorphic chlorite as a petrogenetic indicator mineral, with special regard to greenschist-facies rocks : Canadian Mineralogist, v. 36, p. 713–726.
Zhou, T., and Phillips, G. N., 1994, Sudoite in the Archaean Witwatersrand basin. Contributions to Mineralogy and Petrology, v. 116, p. 352–359.